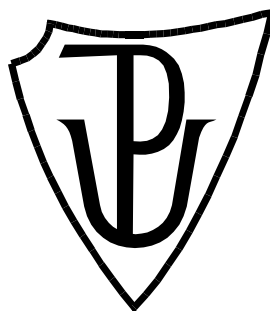


UNIVERZITA PALACKÉHO V OLOMOUCI

Přírodovědecká fakulta

Katedra biochemie



**Regulace pluripotence homeodoménovými
transkripčními faktory v modelové rostlině *Arabidopsis
thaliana***

BAKALÁŘSKÁ PRÁCE

Autor:	Isaac Sugraňes
Studijní program:	B1406 Biochemie
Studijní obor:	Biotechnologie a genové inženýrství
Forma studia:	Prezenční
Vedoucí práce:	Mgr. Yoshihisa Ikeda, Ph.D.
Rok:	: 2021

PALACKÝ UNIVERSITY OLOMOUČ

Faculty of Science

Department of Biochemistry



**Control of plant pluripotency by homeodomain
transcription factors in *Arabidopsis thaliana***

BACHELOR THESIS

Author:	Isaac Sugraňes
Study program:	B1406 Biochemie
Field of study:	Biotechnologie a genové inženýrství
Form of study:	Prezenční
Supervisor:	Mgr. Yoshihisa Ikeda, Ph.D.
Year:	: 2021

Prohlašuji, že jsem bakalářskou práci vypracoval samostatně s vyznačením všech použitých pramenů a spoluautorství. Souhlasím se zveřejněním bakalářské práce podle zákona č. 111/1998 Sb., o vysokých školách, ve znění pozdějších předpisů. Byl jsem seznámen s tím, že se na moji práci vztahují práva a povinnosti vyplývající ze zákona č. 121/2000Sb., autorský zákon, ve znění pozdějších předpisů.

V Olomouci dne

.....

I declare that I am the sole author of this bachelor thesis, indicating all the sources and co-authorship. I agree with the publication of my bachelor thesis according to Act no. 111/1998 Coll., about Universities, as amended. I have been informed that my work is subject to legal rights and obligations arising from the Act no. 121/2000 Coll., the Copyright Act, as amended, are applied to my work.

At Olomouc

.....

Poděkování

Především bych chtěl poděkovat svému vedoucímu Dr. Yishihisa Ikedovi za jeho ochotu, čas mi věnovaný a veškeré rady. Děkuji za všechny znalosti, které mi předal a vše co mě naučil. Chtěl bych také poděkovat Ivoně Kubalové, díky které jsem se dostal na oddělení molekulární biologie. Dále bych chtěl poděkovat Davidovi Zalabákovi za veškeré konzultace. Nakonec bych chtěl poděkovat celému oddělení molekulární biologie za příjemné pracovní prostředí, a oddělení buněčné biologie za poskytnuté vzdělání.

Tato práce byla sponzorována Grantovou agenturou České republiky (GACR17-23702S a GACR 18-23972Y) a IROAST výzkumnou jednotkou rostlinné kmenové buňky a regenerace.

Acknowledgements

First of all, I would like to sincerely thank my supervisor Dr. Yoshihisa Ikeda for his willingness, his time and all the advice. I thank for all the knowledge he provided me and for all he taught me. I'd also like to thank Ivona Kubalová for bringing me to the department of molecular biology. Furthermore, I would like to thank David Zalabák for all consultations provided. Finally, I would like to thank the whole department of molecular biology for comfortable work environment and the department of cell biology for education provided.

This work was supported by Grant Agency in the Czech Republic (GACR17-23702S and GACR 18-23972Y) and IROAST research unit plant stem cells and regeneration.

Bibliografická identifikace

Jméno a příjmení autora	Isaac Sugraňes
Název práce	Regulace pluripotence homeodomenovými transkripčními faktory v modelové rostlině <i>Arabidopsis thaliana</i>
Typ práce	Bakalářská
Pracoviště	Katedra biochemie
Vedoucí práce	Mgr. Yoshihisa Ikeda, Ph.D.
Rok obhajoby práce	2021

Abstrakt

Veškeré nadzemní orgány rostlin se vyvíjí ze stonkového apikálního meristému, což je populace pluripotentních buněk, které se v průběhu života diferencují v tkáň, zatímco je populace meristematických buněk zachována. Rostlina v průběhu života vytváří nové boční meristémy, ze kterých vznikají nové větve a květy. Tato práce se zabývá analýzou vývoje nadzemních meristémů a jeho hormonální a genovou regulací. Praktická část se věnuje genům *WUS*, *ESR* a členům genové skupiny *HD-ZIP III*. V této práci je studován vývoj bočních orgánů nezávisle na *WUS* a dále interakce mezi *HD-ZIP III* a *ESR* geny v přítomnosti *WUS*.

Klíčová slova	SAM, laterální meristém, HD-ZIP III, ESR1/2, WUS
Počet stran	55
Počet příloh	0
Jazyk	Anglický

Bibliographical identification

Autor's first name and surname	Isaac Sugrañes
Title	Control of plant pluripotency by homeodomain transcription factors in <i>Arabidopsis thaliana</i>
Type of thesis	Bachelor
Department	Department of biochemistry
Supervisor	Mgr. Yoshihisa Ikeda, Ph.D.
The year of presentation	2021

Abstract

All above ground organs develop from the shoot apical meristem, which is population of pluripotent cells, that throughout life undergo differentiation to form tissues, whilst the meristematic cell population is maintained. Plant in its lifetime forms new lateral meristems from which new branches and flowers arise. This work deals with analysis of above-ground meristems development and their hormonal and genetic regulation. The practical part is focused on *WUS*, *ESR* and *HD-ZIP III* genes. In this work we studied the lateral organ formation in *WUS*-dependent pathway and interactions between *HD-ZIP III* and *ESR* genes in presence of *WUS*.

Keywords	SAM, lateral meristem, HD-ZIP III, ESR1/2, WUS
Number of pages	55
Number of appendices	0
Language	English

TABLE OF CONTENTS

1	Introduction.....	1
2	CURRENT STATE OF THE TOPIC.....	2
2.1	<i>Arabidopsis thaliana</i> (Mouse-ear cress).....	2
2.2	Shoot apical meristem	2
2.2.1	<i>SHOOT MERISTEMLESS</i> gene	4
2.2.2	Role of <i>WUSCHEL</i> in SAM.....	5
2.3	Auxin signaling in SAM.....	8
2.3.1	Auxin mediated regulation of transcription	8
2.3.2	Auxin transporters.....	10
2.4	Cytokinin signaling in SAM.....	10
2.5	Class III Homeodomain-Leucine Zipper Gene Family.....	12
2.5.1	Patterning of the embryonal apex	14
2.5.2	Role of HD-Zip III genes in postembryonic meristem initiation.....	15
2.5.3	Impact of <i>PHB</i> , <i>PHV</i> and <i>REV</i> on leaf polarity	16
2.5.4	HD-ZIP III activity modulation	16
2.6	AP-2 type transcription factors.....	16
2.6.1	Role of <i>ESR</i> genes in embryo patterning	18
2.6.2	Link between <i>ESR</i> and <i>HD-ZIP III</i> genes	19
2.7	Formation of axillary and floral meristems.....	19
2.8	<i>WUSCHEL</i> independent SAM developmental pathway	22
3	Material and methods.....	24
3.1	Material	24
3.1.1	Plant material	24
3.1.2	Chemicals.....	24
3.1.3	Solutions and culture media.....	25

3.1.4	Enzymes	26
3.1.5	Laboratory equipment and devices	26
3.1.6	Software	27
3.1.7	Primers	27
3.2	Methods	27
3.2.1	½ MS solid medium preparation.....	27
3.2.2	Seed sterilization	28
3.2.3	Plant growing	29
3.2.4	Genomic DNA extraction	29
3.2.5	PCR genotyping	29
3.2.6	DNA electrophoresis	30
3.2.7	DNA restriction.....	31
3.2.8	Plant crossing	31
3.2.9	Phenotypical analysis	32
4	Results.....	33
4.1	Seedling phenotype analysis	33
4.2	Phenotype analysis of mature plants	37
4.2.1	Lateral organ development.....	37
4.2.2	Inflorescence meristem development.....	39
5	Discussion	42
6	Conclusion	45
7	References	46
8	List of abbreviations.....	54

Aims of the bachelor thesis

Theoretical part

Summarize the published knowledge on shoot apical meristem development in *Arabidopsis thaliana*. Identify key players in shoot apical meristem development and

Practical part

Create higher order *HD-ZIP III* mutants together with *ESR* mutants. Create higher order mutants in *wus* mutant background.

Analyze the effects of individual genes in development of lateral meristems in seedlings and in adult plants in different pathways.

1 Introduction

Plants as sessile organisms have to continuously develop new organs throughout their lifespan, passing from vegetative to reproductive phase. The formation of new organs originates in small pluripotent cell populations called meristems. During the embryogenesis two apical meristems are established: shoot apical meristem and root apical meristem. From the shoot apical meristem emerge all the above ground organs. During the vegetative phase new lateral meristems are established from which branching and later in reproductive phase, floral development occurs.

The meristematic cell fate is affected by numerous genes. However major role in meristem development play *WUSCHEL* (*WUS*), *CLAVATA* (*CLV*) and *SHOOT MERISTEMLESS* (*STM*). The formation of lateral organs is though affected also by genes of HD-ZIP III family. The HD-ZIP III members interact with AP2-type transcription factors *ESR1* and *ESR2*.

In this work we focus on the development of the shoot apical meristem and key players in this process. We studied the genetic interactions of *WUS*, *HD-ZIP III* members and *ESRs* in lateral organ formation.

2 CURRENT STATE OF THE TOPIC

2.1 *Arabidopsis thaliana* (Mouse-ear cress)

Arabidopsis thaliana is a small dicotyledonous plant from *Brassicaceae* family that could be found in Asia, Europe and North America with the Columbia and Landsberg ecotypes accepted as standard for studies. The whole life cycle of the plant from the seed germination to the maturation of the first seeds takes six weeks. The plant usually undergoes self-pollination, but the flowers can be crossed by application of pollen to the surface of the stigma. Mature plant can then produce more than 5000 seeds which mature in so called siliques (Meinke et al., 1998).

The genome of *Arabidopsis* consists of five chromosomes with over 25 000 genes. The whole genome size is 125 Mb (The Arabidopsis Genome Initiative, 2000). With the use of *Agrobacterium tumefaciens* mediated transformation transfer-DNA (T-DNA) insertion mutants were prepared for most of the genes (O'Malley et al., 2015). With the expansion of informative technologies online databases emerged. These tools enable us to access the data and the material (Holland and Jez, 2018).

2.2 Shoot apical meristem

During embryogenesis takes place the formation of the root apical meristem (RAM) and the shoot apical meristem (SAM), which are small populations of pluripotent stem cells. The SAM is located at the tip of shoot and gives rise to the whole aerial part of the plant (flowers, leaves, stems and gametes) whilst keeping a reservoir of stem cells for further growth (Bowman and Eshed, 2000). The SAM is derived from epidermal and hypodermal layers of cells in upper hemisphere of globular stage embryo. Cells in the hypodermal layer divide periclinally, resulting in formation of three-layered upper hemisphere at late globular to torpedo stage. In the torpedo stage the SAM emerges from the three layers of cells between folding cotyledons. It has a dome shape and is divided to structural subdomains: The two upper cell layers L1 from epidermal layer and L2 from upper hypodermal layer, together forming the tunica layer. Cells of the tunica layer divide anticlinally, perpendicular to the outer surface. The third layer, L3 (referred to as corpus layer), consists of more than one layer of cells and is derived from the lower hypodermal

cells. These cells divide both anticlinally and periclinally, parallel to the outer surface (Figure 1B) (Satina et al., 1940; Barton and Poethig, 1993).

Histological analysis of the SAM, first being histologically distinct at the transition from globular to heart stage embryo, shows high level of organization. In the center of the surface zone of the meristem is the central zone (CZ) which consists of small population of stem cells that maintain the meristem. The maintenance of central zone is ensured by underlying organizing center (OC). Underneath the organizing center is the rib zone (RZ) that causes stem elongation. Around the central zone is the peripheral zone (PZ) from which organ primordia emerge (Figure 1A) (Murray et al., 2012).

Stem cells are undifferentiated cells that retain the ability to divide. Part of the daughter cells remain the character of stem cells and the rest differentiates into specialized cells. The more the cell gets differentiated the lower is the ability to proliferate and give rise to different cell types. Stem cells are kept in a niche which provides maintenance

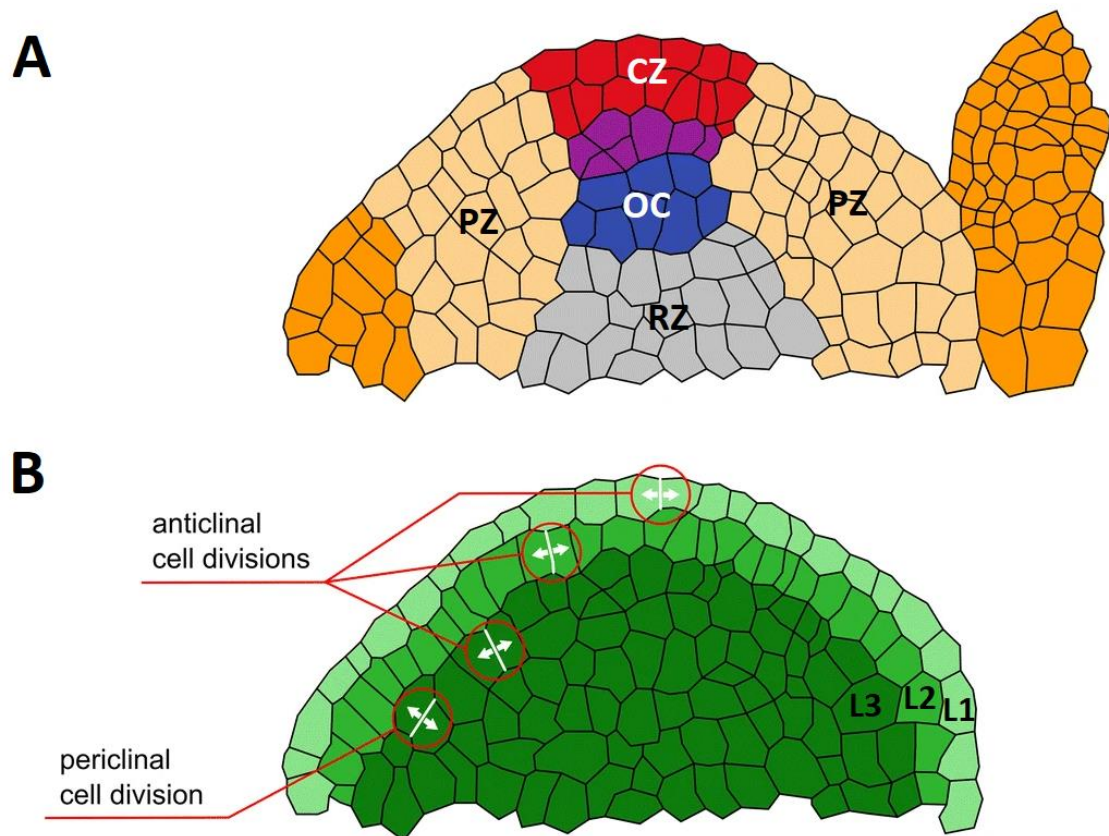


Figure 1 A: Schematic representation of SAM. Central zone (CZ) - red, organizing center (OC) - blue, peripheral zone (PZ) - pink, rib zone (RZ) - gray, organ primordia – orange, overlap of CZ and OC – purple. B: Representation of L1 – light green, L2 – darker green, L3 – darkest green, SAM layers with representation of cell divisions. Adapted from (Fuchs and Lohmann, 2020) and edited.

signals to the stem cells. Once the stem cell leaves the niche it loses stem cell identity and progresses to differentiate (Fuchs and Lohmann, 2020).

The stem cells are concentrated in the central zone and during cell proliferation are the surrounding cells pushed either laterally to the peripheral zone or basally to the rib zone. Central zone is specific by expression of *CLAVATA3* gene (*CLV3*) (Fletcher et al., 1999). Cells situated at the periphery divide faster and in response to auxin signaling they start to differentiate as they are more distant from the CZ. After cells leave the meristem they become part of organ primordia from which leaves or flowers are formed (Meyerowitz, 1997; Reddy et al., 2004).

2.2.1 *SHOOT MERISTEMLESS* gene

SHOOT MERISTEMLESS (*STM*) gene plays an important role in SAM function. It encodes 328 residues long protein homologous to KNOTTED class homeodomain transcription factors (Long et al., 1996). *stm-1* allele was isolated by EMS mediated mutagenesis. The *stm-1* homozygous mutant plants have arrested development of SAM at or after torpedo stage of embryonal development and therefore don't form a SAM (Barton and Poethig, 1993). The *stm* seedlings can produce leaves from the fused part of cotyledonary petioles and subsequently leaves emerge from petioles of those formed leaves. Root explants of *stm* seedlings, although being able to form leaves, failed to produce inflorescence on shoot inducing medium, indicating that *STM* is required for SAM initiation in both embryonal and postembryonal development (Barton and Poethig, 1993; Endrizzi et al., 1996).

Weaker *stm* alleles showed laves and cotyledon fusions during development. The *stm* mutation was shown to be epistatic to mutation in *WUSCHEL* (*WUS*) gene, indicating that *STM* acts upstream of *WUS* (Endrizzi et al., 1996). The *stm* shoot meristems are terminated by "consumption" of stem cells by incorporation into ectopic organ primordia and differentiation, leading to flat enlarged apices. *STM* is therefore continuously required for SAM maintenance after globular embryo stage. (Endrizzi et al., 1996; Clark, 1997). In globular embryo *STM* is expressed in cells predicted to form embryonic SAM, between cotyledon primordia at heart stage to mature embryo and in vegetative, axillary, inflorescence and floral meristems later in development, supporting the role of *STM* in SAM maintenance (Long et al., 1996). A weak *stm-2* allele was identified, where *stm-2* mutants form shoot meristems between cotyledons that terminate after initiation of

several primordia, further supporting the role of *STM* in maintenance of undifferentiated cells in the SAM (Clark et al., 1996).

STM appears to have opposite function to *CLAVATA 1* and *3* (*CLV1*, *CLV3*) genes, which promote differentiation of SAM cells and restrict their proliferation. *clv* mutants form a SAM with large pool of undifferentiated cells (Clark et al., 1995). *stm-1* mutants heterozygous for either *clv1* or *clv3* develop leaves more often and faster than *stm-1* only, this effect is increased in *clv stm-1* homozygous double mutant (Clark et al., 1996). Additionally *clv stm-1* double mutants forms inflorescences, often with fasciated stems as seen in *clv* (Clark et al., 1993, 1996). The heterozygous *stm* mutation also partially rescues the *clv* mutant phenotype of gynoecium. This indicates that *stm* and *clv* mutants require wild-type levels of *CLV* and *STM* activities respectively to manifest their phenotypes (Clark et al., 1996).

STM is expressed in a continuous band between cotyledons at heart stage embryo, playing role in cotyledon separation. (Long and Barton, 1998) The *stm* phenotype of partially fused cotyledons is similar to that of mutants in *CUP-SHAPED COTYLEDON 1* and *2* (*CUC1*, *CUC2*), involved in formation of the SAM and separation of cotyledons (Aida et al., 1997). The *cuc1 cuc2* double mutant show absence of embryonal SAM and almost completely fused cotyledons, leading to cup-shaped cotyledon phenotypes, as a result of bulging of boundary region of cotyledon margins at heart stage. The fusion of cotyledon petioles in *stm* mutants is caused by bulging in the same area at the bending-cotyledon stage later in development (Aida et al., 1999). The double mutants are occasionally capable of adventitious shoot formation from hypocotyl tissue culture with almost normal vegetative and reproductive development, indicating that *CUC1* and *CUC2* aren't essential for maintenance of the SAM (Aida et al., 1997). It was shown that *STM* expression is dependent on *CUC1* and *CUC2* and that *CUC2* proper spatial expression at the bending cotyledon stage depends on *STM*. *stm* mutation combined with one *cuc* mutation results in enhancement of cotyledon fusion phenotype, indicating that the genes act in and overlapping pathway (Aida et al., 1999).

2.2.2 Role of *WUSCHEL* in SAM

The *WUSCHEL* (*WUS*) gene was first identified in genetic screen following EMS mutagenesis where homozygous *wus* mutant can't maintain shoot meristems. The gene is situated on the chromosome 2 in *A. thaliana*. The adult *wus* mutant phenotype is

characterized by large number of rosette leaves clustered of the base of the plant, therefore the name (from German *Wuschelkopf* – person with fuzzy hair). Flowers are formed rarely in this mutant and if present are generally infertile. (Laux et al., 1996).

The gene codes a 291 amino acids protein with two main functional domains: first domain of 66 amino acids with function of DNA binding homeodomain similar to known homeodomains (Mayer et al., 1998). The second domain is a cluster of acidic amino acid residues predicted to form structure associated with transactivation domains (Fuchs and Lohmann, 2020). *WUS* was localized in epidermal cells nuclei therefore was classified as homeodomain transcription factor (Mayer et al., 1998).

In the organizing center *WUSCHEL* (*WUS*) is expressed as a key stem cell regulator in SAM. The *WUS* mRNA is accumulated in cells in center of L3 and in lower layers but not in the L1 and L2 of central zone thus *WUS* was said to act non-cell autonomously, affecting the upper layers (Laux et al., 1996).

WUS orthologs were identified in different plant species and led to identification of two conserved motifs: TLPLFPMH motif called *WUS* box which function remains unknown (Haecker et al., 2004) and EAR-like domain which have been previously shown to act as transcriptional repressors. Both EAR-like domain and acidic domain of *WUS* box are located on the C-terminus of the protein which is necessary to rescue the *wus* phenotype (Kieffer et al., 2006). Acidic domain of *WUS* was proven to activate transcription while EAR-like domain acts as repressor similarly to *WUS* box. The *WUS* box being crucial for biological function of *WUS* (Ikeda et al., 2009).

2.2.2.1 *CLAVATA3/WUSCHEL* feedback loop

WUS activates and maintains the expression of *AGAMOUS* (*AG*) gene which is expressed in the floral meristem that acts as regulator of floral stem cells proliferation and organ identity of the flower. *ag* mutant flowers produce sepals, petals and chimeric structures of the two but are unable to grow carpels and stamen (Lohmann et al., 2001). The number of sepals and petals varies in this mutant (Bowman et al., 1989). On the other hand, *wus* doesn't produce either carpels and stamens but the number of petals and sepals is normal. The double mutation in both genes led to growth of flowers with sepals and a central petal (Laux et al., 1996). *WUS* was shown to establish *AG* expression in floral meristem and to activate *AG* transcription through direct binding to its promoter. *AG* protein then acts as

negative regulator of *WUS* to prevent over-accumulation of floral stem cells, thus forming a feedback loop (Lohmann et al., 2001).

In analogy *WUS* plays part in feedback loop with *CLAVATA3 (CLV3)*. *CLV3* is a small peptide secreted by the stem cells in the CZ. It promotes differentiation of other stem cells in non-cell autonomous manner (Clark et al., 1995, p. 3). *WUS* induces expression of *CLV3*, *CLV3* then acts as repressor for *WUS*. Increased expression of *WUS* then leads to higher expression of *CLV3* which then leads to decreased expression of *WUS* that causes lower expression of *CLV3*. By this feedback loop is regulated the pool size of stem cell population and its balance with differentiation. *clv3* mutation results in increased expression domain of *WUS*, thus in meristem over proliferation (Brand et al., 2000).

wus mutant shows no expression of *CLV3* in the embryo but is expressed later during development through induction by homeodomain transcription factor *SHOOT MERISTEMLESS (STM)* (Brand et al., 2002). *CLV3* positive cells are not maintained and undergo differentiation (Laux et al., 1996).

2.2.2.2 WUSCHEL and hormonal signaling

Plant hormones are very important for stem and root development. *WUS* directly acts as repressor of transcription of *ARABIDOPSIS RESPONSE REGULATORS (ARR7 and ARR15)*. These are induced by cytokinin, but they negatively regulate the cytokinin signaling pathway. Overexpression of *ARR7* leads to seedling phenotypes similar to *wus* mutants (Leibfried et al., 2005). Cytokinin signaling mediated by *ARR7/ARR15* activates *WUS* expression in feedback loops dependent on *CLV* and also in *CLV*-independent manner (Gordon et al., 2009). Auxins' role is negative regulation of *ARR7* and *15* through *AUXIN RESPONSE FACTOR 5/MONOPTEROS (MP)*. N-1-naphthylphthalamic acid (NPA) inhibits auxin transport which causes increase of *CLV3* expression, thus decrease of *WUS* expression. Therefore, auxin and cytokinin play role in stem cell development by affecting *ARR7/ARR15* which has impact on the *CLV3/WUS* feedback loop (Zhao et al., 2010).

2.2.2.3 WUSCHEL protein transport

The intercellular movement of proteins have been previously proven in case of *STM* which is also homeobox protein like *WUS* which led to the idea that *WUS* is also a mobile protein (Kim et al., 2003; Yadav et al., 2011). *WUS* mRNA was located in the OC, but

the WUS protein was located in L1 and L2 of the SAM. The blockage of plasmodesmata in *CLV3* positive stem cells resulted in early differentiation and precocious disappearance stem cells. Additionally, when plasmodesmata were blocked the WUS was restrained only to the OC. This showed the importance of plasmodesmata in stem cell maintenance. It was also concluded that intercellular mobility of WUS isn't dependent on SAM tissue specific proprieties but that it's a specific propriety that is encoded within its sequence. The most important mobility restricting sequence turned out to be amino acids 100-249 between the homeodomain and the WUS box of the WUS protein (Daum et al., 2014). This sequence has an overlap with a sequence involved in homodimerization (amino acids 117-292) (Busch et al., 2010). Two sequences responsible for homodimerization were described, namely homodimerization domain 1 (HOD1) and HOD2. WUS protein Mutation in both domains caused reduction in dimerization and these mutants couldn't rescue *wus* phenotype. It was suggested that WUS DNA binding and homodimerization are necessary for WUS to accumulate in the nuclei and for spatial distribution of WUS in the SAM. When only the first 134 amino acids containing HOD1 were kept while the C-terminus was spliced out, WUS was distributed uniformly in the meristem, implicating that the C-terminal region contains information for spatial distribution. At the same time only the 63 C-terminal amino acids showed similar distribution as endogenous WUS. Hence the last 63 amino acids are responsible for WUS distribution (Rodriguez et al., 2016).

2.3 Auxin signaling in SAM

Auxin is plant hormone responsible for coordination of development and growth. It can transfer information over variable ranges. Specific for auxin are its different functions of different cells depending on the auxin level changes. The effect of auxin on cells is dependent on the signal perceiving cell and its predetermined identity and also depends on absolute and relative levels on auxin at given location (Leyser, 2018). Auxin regulates growth coordination function in terms of spatio-temporal growth of tissue depending on the conditions (Bennett and Leyser, 2014).

2.3.1 Auxin mediated regulation of transcription

Auxin levels changes cause cellular response by affecting transcription via signal transduction pathway where auxin unites members of the Aux/IAA transcriptional repressor family with F-box proteins of the TRANSPORT INHIBITOR

RESPONSE1/AUXIN SIGNALING F-BOX (TIR1/AFB) family. F-box proteins are subunit of SCF-type ubiquitin protein ligase complexes: Skp1, Cullin and F-box protein. SCF is responsible for target protein ubiquitination (Tan et al., 2007). The formed TIR1/AFB-Aux/IAA pairs form a coreceptor for auxin. Changes in levels of auxin are converted into Aux/IAA levels changes by bringing TIR1/AFB-Aux/IAA to the SCF, causing their ubiquitination and degradation (Maraschin et al., 2009).

Aux/IAAs act as transcriptional repressors while they recruit transcription corepressors of the TOPLESS (TPL) family to promoters through their EAR domain, The TPL proteins can activate chromatin remodeling proteins to stabilize repression of transcription (Szemenyei et al., 2008). Aux/IAA proteins don't have DNA binding domain, but they form dimers with AUXIN RESPONSE FACTOR (ARF) family through C-terminal PB1 domain common to the two protein families. The PB1 domain dimerizes via acidic and basic interaction surfaces (Guilfoyle, 2015, p. 1). ARF proteins also homodimerize by their B3 domain located at the N-terminus, this leads to formation of ARF homodimers that cooperatively bind DNA (Boer et al., 2014). ARFs bind to Auxin Response Elements (AREs) in promoters of auxin inducible genes (Mironova et al., 2014). ARFs that include Q-rich middle domain between B3 and PB1 domains can activate transcription by recruiting chromatin remodeling enzymes. When oligomerized with Aux/IAA the transcription activation is inhibited. Many ARFs lack the Q-rich region and there is evidence they act on AREs as transcriptional repressors (Ulmasov et al., 1997). This reveals a mechanism by which varies the response to auxin signaling in different cell types. The oligomerization of Aux/IAAs together could prevent binding to ARFs, therefore activate transcription (Leyser, 2018). A synthetic auxin responsive DR5 promoter has been produced. It consists of minimal promoter fused with seven ARE repeats. It is used in fusion with reporter genes to study auxin distribution at cellular level (Chen et al., 2013).

The transcription is affected very quickly by auxin signaling, while changes in transcript levels are detected within 5 minutes of auxin treatment. The half-life of most Aux/IAAs is very short and their transcription is upregulated by auxin (Abel and Theologis, 1996). This indicates that auxin modulates transcription in highly dynamic, feedback regulated network where gene expression is dependent on the Aux/IAA degradation-synthesis cycle (Bridge et al., 2012).

2.3.2 Auxin transporters

The polar auxin transport has been shown to play role in establishment of apical-basal polarity and also bilateral symmetry (Friml et al., 2003; Liu et al., 1993). In the SAM auxin is transported intercellularly through PIN family of functionally redundant auxin efflux carriers. The primordia emerge at the sites of locally high auxin concentration in the PZ (Reinhardt et al., 2003). Auxin itself causes the polar PIN accumulation by affecting its transcription (Hazak et al., 2010). The auxin concentration gradient is due to polar PIN1 orientation toward cell with higher intracellular auxin concentration (Smith et al., 2006). This noncell-autonomous polarization depends on the TIR1/AFB-Aux/IAA system. In the SAM the ARF MONOPTEROS (MP) is a key player in organ emergence patterning. The MP protein contains nuclear localization sequences as well as a DNA binding domain capable of binding to auxin inducible promoters (Hardtke and Berleth, 1998). Expression of *MP* is controlled by auxin and causes PIN1 polar orientation (Bhatia et al., 2016). *MP* encodes ARF5 and *BODENLOS* (*BDL*) encodes its inhibitor IAA12 (Hamann et al., 2002; Ulmasov et al., 1999). Also a serine/threonine protein kinase encoded by *PINOID* (*PID*) gene was identified, affecting PIN proteins localization (Benjamins et al., 2001; Bennett et al., 1995).

Higher-order *pin* mutants display post embryonically reflected embryonic cell division defects in cotyledon development, resulting in fusion of cotyledons or presence of single cotyledon (Furutani et al., 2004). Moreover *mp*, *bdl* and *pid* mutants all showed defects in cotyledon development (Bennett et al., 1995; Hardtke and Berleth, 1998; Ulmasov et al., 1999).

2.4 Cytokinin signaling in SAM

Cytokinins are plant hormones that promote cell division and differentiation (Skoog and Miller, 1957). They play role in seed germination, embryogenesis, SAM and RAM development, vasculature formation and leaf senescence (Hwang et al., 2012). The natural cytokinins are derivatives of adenine (Mok and Mok, 2001). ISOPENTENYL TRANSFERASE (IPT) was defined as enzyme responsible for cytokinin biosynthesis (Sa et al., 2001; Takei et al., 2001). The cytokinin signaling is a phosphorelay pathway, often present in bacteria, consisting of two conserved proteins: His kinase sensor, consisting of input domain and conserved transmitter domain, and response regulator protein. Input domain perceives the signal and then modifies the transmitter domain. His residue of

transmitter domain of His kinase and Asp residue of response regulator receiver domain are phosphorylated (West and Stock, 2001; Hwang et al., 2002). Many response regulators contain a second, output domain, regulated by receiver domain phosphorylation, acting as transcription factor (West and Stock, 2001). In *Arabidopsis* His kinases (AHKs) act as phytochrome, ethylene and cytokinin receptors (Schaller, 2000). *Arabidopsis* response regulators (ARRs) containing Arg and *Arabidopsis* His phosphotransfer proteins (AHPs) were identified in cytokinin signaling pathway (Suzuki et al., 1998; Schaller et al., 2008). Several of AHKs contain a C-terminal receiver domain. AHK2, AHK3 and AHK4/CRE1 contain between the transmitter domain and the C-terminal domain an additional receiver domain lacking some of highly conserved residues (Ueguchi et al., 2001).

The cytokinin pathway is initiated by autophosphorylation at His-residue in the N-terminal sensor-kinase domain of hybrid His kinases. The signal is transferred by phosphorylation at Asp of the C-terminal receiver domain (Hwang and Sheen, 2001). Cytokinins bind to the transmembrane CHASE (cyclases/histidine kinases-associated sensory extracellular) domain of AHK2, 3 and 4 (Anantharaman and Aravind, 2001; Mougel and Zhulin, 2001). The *CYTOKININ-INDEPENDENT1 (CKII)* gene encoding protein with similar sequence to His kinases was identified (Kakimoto, 1996). The CKII protein when overexpressed can activate the whole cytokinin signaling pathway. The signal is transmitted through AHPs to the nucleus (Hwang et al., 2002). The nuclear type-B ARR promotes the expression of nuclear type-A ARR, acting in negative regulation of cytokinin signaling, thus they act in a negative-feedback loop (Hwang and Sheen, 2001; Sakai et al., 2001; Argueso et al., 2010).

The ratio between auxin and cytokinin levels is crucial for proper development. Whereas relative abundance of auxin leads to *de novo* establishment of root identity, abundance of cytokinin causes shoot development (Skoog and Miller, 1957). In embryogenesis is cytokinin signaling first apparent in hypophysis. Later at the heart stage is cytokinin signaling restricted to the stem-cell precursors (Müller and Sheen, 2008). In the SAM the cytokinin signaling is established after expression of *STM* and *WUS* (Aichinger et al., 2012). *WUS* acts in repressing transcription of various A-type *ARRs*, causing increased cytokinin perceptivity (Leibfried et al., 2005). Further AHK2 and AHK4 repress *CLV1* expression which ultimately leads to increased *WUS* expression. *WUS* is also upregulated by cytokinin signaling in *clv1* mutants, showing its direct effect

on *WUS* expression. Thus a positive-feedback loop exists between *WUS* and cytokinin signaling, supported by high cytokinin signaling activity in *WUS* expressing domain (Gordon et al., 2009). Similar positive-feedback loop is applied for *STM*, inducing *IPT7* transcription, therefore promoting cytokinin synthesis. Cytokinin signaling causes activation of *STM* transcription (Yanai et al., 2005). Enhancement of cytokinin action stimulates SAM activity and loss of cytokinin signaling leads to reduction of SAM size, which supports role of cytokinin in SAM development (Nishimura et al., 2004; Bartrina et al., 2011). Cytokinins have been shown to induce proliferation in SAM, probably by their positive effect on genes promoting cell cycle (Riou-Khamlichi et al., 1999). It was also demonstrated that cytokinin signaling affects arrangement of lateral meristems and phyllotaxis (Giulini et al., 2004; Zhao et al., 2010).

2.5 Class III Homeodomain-Leucine Zipper Gene Family

Approximately 65% of *A. thaliana* genes belong to gene families (The Arabidopsis Genome Initiative, 2000). The whole HD-Zip family can be classified into four subfamilies by different DNA-binding specificities, gene structures, common motifs and physiological functions (Ariel et al., 2007). Class III Homeodomain-Leucine Zipper (HD-Zip III) gene family are highly conserved in land plants. The family consists of *CORONA (CNA)*, *PHABULOSA (PHB)*, *PHAVOLUTA (PHV)*, *REVOLUTA (REV)* and *HOMEBOX8 (ATHB8)* (Figure 4) (Prigge et al., 2005). HD-ZIP III proteins contain five functional domains. The first two are homeodomain (HD) linked closely to leucine zipper motif (Zip) responsible for DNA binding and dimerization respectively. HD-Zip proteins bind DNA as dimer and in the absence of the Zip motif the proteins are unable of the DNA binding (Ariel et al., 2007). The other three domains are steroidogenic acute regulatory protein lipid transfer (START) domain, homeodomain-START associated domain (HD-SAD) and a C-terminal MEKHLA domain (Figure 2) (Sessa et al., 1993; Mukherjee and Bürglin, 2006).

These genes mRNAs are targets of microRNAs (miRNAs) from *miR165/166* group. miRNAs are 20-24 bp long single stranded RNAs that base pair with target mRNAs to inhibit their transcription or to cleave those target mRNAs via RNA-induced



Figure 2 Schematic representation of HD-ZIP III protein domains. Adapted from (Ariel et al., 2007)

silencing complex (RISC) (Bartel, 2004). miRNAs are processed from double-stranded regions of larger RNAs by the action of RNases family *DICER-LIKE* and *ARGONAUTE* gene family (Bao et al., 2004; Reinhart et al., 2002). miRNAs are essential for plant development, which is supported by lethal phenotype of *dcl1*, that is unable to produce miRNAs (Schauer et al., 2002). Plant miRNAs are characteristic by their almost full complementarity with their targets (Rhoades et al., 2002). The binding site of miR165/166 is the highly conserved START- coding domain (Williams et al., 2005). The gain-of-function mutants in *HD-ZIP III* genes, having mutation in miRNA binding regions, are resistant to cleavage mediated by these miRNAs that results in the increased expression of these transcription factors. It was suggested that miRNAs cause chromosomal methylation downstream of miRNA binding site, resulting in lower expression (Bao et al., 2004). It has been also shown that transcription inhibition occurs at rough endoplasmic reticulum (Li et al., 2013). A zinc finger protein SERRATE (SE) was described to play role in processing of pri-miR165/166, thus affecting expression of *HD-ZIP III* genes. The mutation in *SE* produces similar phenotypes to those of gain-of-function mutants *phb-1d* and *phv-1d* (Grigg et al., 2005). Similarly a gain of function mutant of *CNA* with single nucleotide transition in START-coding domain *icu4* is also a gain of function semi-dominant mutant resistant to miRNA characterized by the upward curled leaves phenotype (Figure 3) (Ochando et al., 2006). Additionally a *jabba-1D* (*jba-1D*) mutant have been characterized by *miR166g* overexpression causing suppression of *PHB*, *PHV*, *CNA*, activation of *REV* but doesn't affect *ATHB8* (Williams et al., 2005). The *jba-1D* phenotype is characteristic by radialized downward curled leaves with

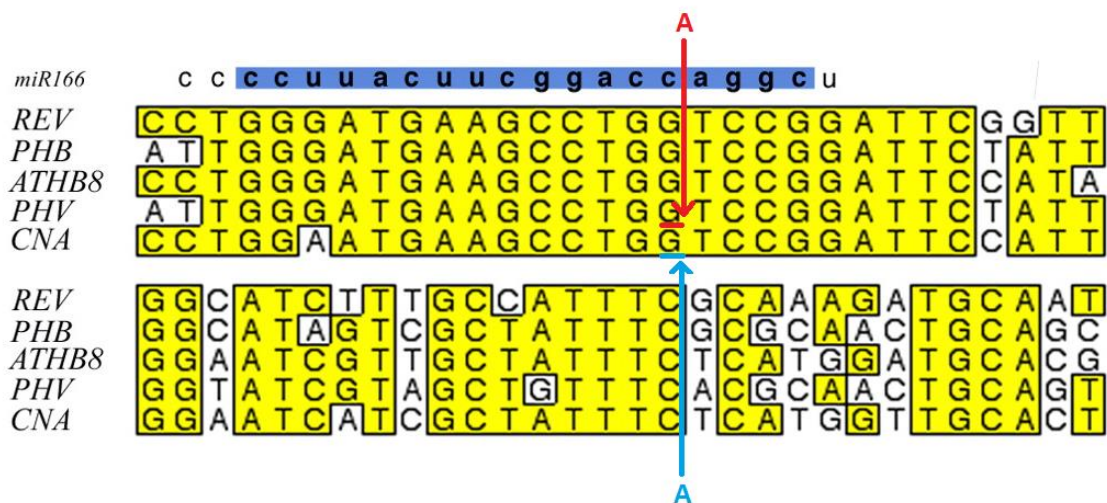


Figure 3 miRNA complementary sequences of *HD-ZIP III* genes with transitions indicated for gain-of-function mutants *icu-4d* (blue) and *phv-1d* (red). Adopted from (Williams et al., 2005) and edited.

adaxial character, fasciated inflorescence meristems and filamentous siliques. The phenotype is dose-dependent, therefore homozygous mutant depicts stronger phenotype. The mutant seedlings form multiple, enlarged SAMs during post-embryonic development. This is caused by enlarged expression domain of *WUS* and *CLV3* that leads to increase in stem cell population. Moreover the *WUS* expression is necessary for the manifestation of *jba-1D* phenotype (Williams et al., 2005).

2.5.1 Patterning of the embryonal apex

CNA, *PHB*, *PHV* and *REV* regulate patterning in the apical part of the embryo. *REV* is specifically expressed in most of embryonic development, but *rev* mutants show no embryonic phenotypes, whereas only *rev* single mutants among the whole family show distinctable phenotypes in mature plant with narrow leaves and malformation of axillary meristems. The role of *REV* in embryonal development is then unclear, but has been shown to promote adventitious shoots postembryonically (Otsuga et al., 2001). *PHB*, *PHV* and *REV* have overlapping roles in establishment of the SAM and in establishment of bilateral symmetry. *rev phb* double mutants show a phenotype, where the SAM is undeveloped, and cotyledons show patterning defects or are absent. Later, in place where SAM is normally located emerges radially symmetric structure with no further growth. In *rev phv* double mutants is the absence of the SAM rare, indicating that role of *PHV* in this process is minor. Although additional mutations in *PHV* or *CNA* in *rev phb* lead to enhancement of the embryo patterning defects. The apical portion of the embryo is replaced by radially symmetric structure in *rev phb phv* triple mutant similarly to *rev phb cna* mutant. The mutation in *ATHB8* doesn't change the *rev phb* double mutant

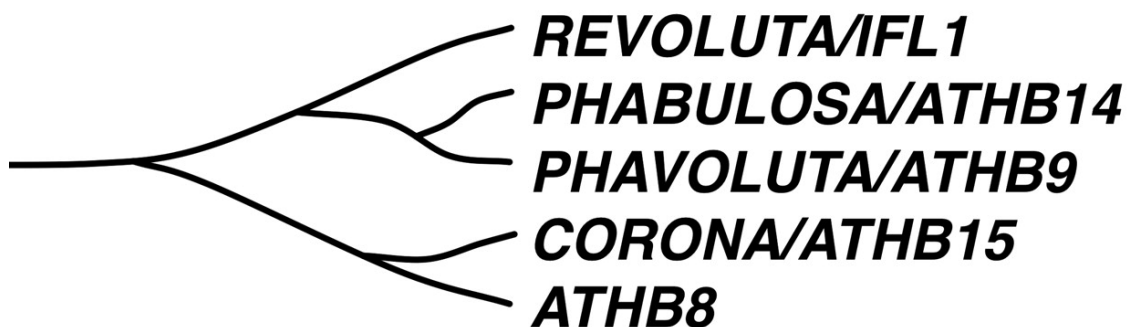


Figure 4 Phylogram of HD-ZIP III genes showing their relations. Adapted from (Prigge et al., 2005).

phenotype. The radially symmetric structure appears to be fully abaxialized radially symmetric cotyledons (Prigge et al., 2005).

2.5.2 Role of HD-Zip III genes in postembryonic meristem initiation

All HD-Zip III members have been shown to regulate meristem initiation postembryonically. *REV* has a major role in formation of lateral shoot meristems, adventitious shoots and floral meristems. *rev* mutants produce cauline leaves and rosettes without axillary meristems and flowers without meristematic activity (Otsuga et al., 2001). The introduction of heterozygous *PHB* mutation in *rev* mutant background enhances the *rev* phenotype and leads to production of small number of fertile flowers. The *rev phv* plants shows similar floral meristem phenotype (Otsuga et al., 2001).

rev cna and *rev athb8* double mutants have similar phenotypes as *rev* single mutant, but the *rev cna athb8* triple mutant produces more fertile flowers and lateral shoot meristems than the single mutant *rev*. Thus, *CNA* and *ATHB8* have antagonistic function to that of *REV* in terms of floral and lateral shoot meristems formation. Mutations in both genes also resulted in partial suppression of *rev phv* floral meristems, where in quadruple mutants this led to formation of fertile flowers (Prigge et al., 2005). In the *jba-1D* mutant the *PHB*, *PHV* and *CNA* expression is reduced whilst *REV* expression is increased, suggesting that *REV* might be negatively regulated by *PHB/PHV/CNA* (Williams et al., 2005).

phb phv and *cna athb8* double mutants exhibit phenotype identical to that of wild-type plants (Prigge et al., 2005). The *phb phv cna* triple mutant on the other hand produces enlarged SAM, extra cotyledons, fasciated stems and flowers with extra organs, similarly to *clv* mutants, and with low fertility due to defects in ovular development (Prigge et al., 2005; Lee and Clark, 2015). The *phb phv cna* phenotype is also very similar to that of *jba-1D* (Williams et al., 2005). It was suggested that *PHB/PHV/CNA* may limit *WUS* expression through *CLV/WUS* pathway (Lee and Clark, 2015). The introduction of heterozygous *REV* mutation or homozygous *ATHB8* mutation in the triple mutant background doesn't significantly affect the phenotype. Therefore, it was hypothesized that the role in meristem regulation of *PHB*, *PHV* and *CNA* doesn't depend on *REV* and *ATHB8* (Prigge et al., 2005).

2.5.3 Impact of *PHB*, *PHV* and *REV* on leaf polarity

Early in leaf primordia development they become polarized along adaxial/abaxial axes, where the adaxial portion of the primordium is proximally to the center of the meristem and later becomes the upper surface of the leaf. The abaxial portion is distally from the meristem and becomes the lower part of the leaf (Carraro et al., 2006). The establishment of adaxial/abaxial polarity is essential for shoot development. It plays role in leaf blade formation, cellular specialization of superior and inferior surfaces of the leaf and in axillary and also shoot apical meristem formation (Otsuga et al., 2001; Eshed et al., 2004).

It has been previously shown that *PHB*, *PHV* and *REV* act redundantly in adaxial cell fate in leaf primordia (Emery et al., 2003). More than 30 % of *rev phv* plants produced at least one trumpet-shaped leaf with adaxial tissue inside the cone and abaxial tissue on the outer surface proximally and normal adaxial/abaxial polarity in the distant portion of the leaf. Introduction of heterozygous *PHB* mutation into the double mutant background caused that almost all leaves were trumpet-shaped. *rev phb phv* mutation is lethal for the seedling (Prigge et al., 2005).

2.5.4 HD-ZIP III activity modulation

Family of *LITTLE ZIPPER* (*ZPR*) genes that are transcriptionally upregulated by activity of HD-ZIP III was described (Wenkel et al., 2007). The *ZPR* proteins contain leucine zipper domain similar to that in HD-ZIP III proteins by which they repress HD-ZIP III activity. *ZPR* proteins prevent HD-ZIP III proteins from forming homodimers necessary for DNA binding, resulting in non-functional heterodimers. This is supported by the same phenotype of loss-of-function mutants of *HD-ZIP III* and plants overexpressing *ZPR* (Wenkel et al., 2007; Kim et al., 2008). Overexpression of *ZPR3* exhibits reduced growth, downward curled leaves and meristem malformations (Kim et al., 2008). All HD-ZIP III members interact with *ZPR3*, as with other *ZPRs* (Wenkel et al., 2007; Kim et al., 2008). Inactivation of *ZPR3* and *ZPR4* leads to disruption of meristematic activities of SAM and axillary meristems (Kim et al., 2008). *PHB* was shown to positively regulate *ZPR3* expression, therefore forming a negative feedback loop (Wenkel et al., 2007).

2.6 AP-2 type transcription factors

High cytokinin/auxin ration in media is used to promote shoot development from callus cultures (Skoog and Miller, 1957). Firstly, a gene *ESR1* (*ENHANCER OF SHOOT*

REGENERATION) was identified for its capability of shoot generation from root cultures when overexpressed even in the absence of cytokinins. This may be caused by increased sensitivity to low endogenous cytokinin levels (Banno et al., 2001).

The *ESR1* protein encoded by the gene located on the 1st chromosome is 328 amino acids long and contains a domain homologous to AP2/EREBP domain of transcriptional factors found in higher plants (Okamoto et al., 1997). *ESR1* overexpression induces initiation of shoot regeneration (therefore the name) but interferes with subsequent differentiation of plant cells. Its expression is induced by cytokinin signaling in *A. thaliana* wild-type and increase in its expression induced by cytokinin occurs at early stages of shoot regeneration in calli (Banno et al., 2001). It was stated that *ESR1* could be involved in maintenance of cell identity in organogenesis or in transition from vegetative growth to organogenic development (Ikeda et al., 2006).

A more active paralogue of *ESR1* in terms of shoot regeneration in tissue culture was identified and named *ESR2* (Ikeda et al., 2006). It was also published that this gene affects meristem cell fate and lateral organ development, where the gene was named *DORNRÖSCHEN-LIKE (DRNL)* (Kirch et al., 2003). Knock down mutation in this gene led to finding of its direct downstream target *CUP-SHAPED COTYLEDON1 (CUC1)*, a NAC domain transcriptional factor promoting adventitious shoot formation (Hibara et al., 2003). Knocked-down expression of *ESR2* displays same phenotype as *cuc1* single mutant. Additionally *CUC1* and *cuc1* transcripts were elevated in *ESR2* overexpressing wild type and mutant plants respectively (Aida et al., 1997; Ikeda et al., 2006).

ESR1 and *ESR2* are most closely related AP2 domain-containing proteins with significant similarity within this domain (Alonso et al., 2003). Both genes being capable of shoot regeneration when overexpressed, but *ESR2* manifesting higher effectivity. *ESR2* expression was observed in leaf primordia, in young cotyledons during embryogenic heart stage and later in walking stick stage was expressed in cotyledon tips and sometimes in the SAM (Ikeda et al., 2006).

Cytokinin signaling comprises of sensor histidine kinases (*AHKs*), phosphotransmitters containing histidine (*AHPs*) and response regulators (*ARRs*) (Hutchison and Kieber, 2002). A-type *ARRs* play role in down-regulation of cytokinin response, while some are induced by cytokinin. B-type on the opposite directly activates cytokinin responsive genes (Sakai et al., 2001). Cytokinin promotes the expression of

class I *KNOX* homeobox genes, including *STM* and also *WUS*, both required for meristem specification and maintenance (Rupp et al., 1999; Bäurle and Laux, 2005).

Plants overexpressing either *ESR1* and *ESR2* manifested similar phenotypes as cytokinins overproducing mutants, suggesting induction of genes in cytokinin biosynthetic pathways by both genes in analogy to *STM* (Ikeda et al., 2006; Yanai et al., 2005). *CRE1/AHK4* is cytokinin receptor gene encoding histidine kinase, having function of cytokinin receptor (Inoue et al., 2001). When *ESR1* and *ESR2* are induced in *cre1/ahk4* mutant it results in shoot regeneration in the absence of cytokinin, rescuing the mutant phenotype. This indicates that both *ESR* genes act in cytokinin independent pathway or downstream of cytokinin signaling pathway (Ikeda et al., 2006).

2.6.1 Role of *ESR* genes in embryo patterning

Angiosperm development has two phases: embryonic phase when primary body plan is established with its two axes of symmetry and postembryonic phase when shoot and root meristems are established. At the transition from globular to heart stage in embryonic development cotyledons are formed, indicating beginning of organogenesis and radial to bilateral symmetry change (Mayer et al., 1991). SAM together with cotyledons emerge from the upper tier of cells in embryonal octant stage (Harada, 1999).

ESR1 is expressed in two to four cell stage of the embryo proper, later in lobes of emerging cotyledons and then from mature heart stage until embryo maturity being restricted in SAM. In postembryonic development is *ESR1* expressed in L1 layer of the SAM, extending to emerging lateral organs (Kirch et al., 2003). *ESR2* expression is observed first in early globular stage, then in its apical portion. In heart stage it is expressed at cotyledon primordia and later in subepidermal cells at the tip of cotyledons. After heart stage *ESR2* expression isn't observable (Chandler et al., 2007).

Four mutant alleles of *ESR* genes have been isolated: *esr1-1* and *esr1-2* insertion mutant alleles for *ESR1*; *esr2-1* insertion allele and *esr2-2* nucleotide substitution allele in AP2 DNA binding domain, causing inability to properly bind target DNA for *ESR2*. *esr1* mutants show abnormal cell division from the globular stage, resulting in malformation of hypophysis region or the suspensor region. Both *esr1* and *esr2* single mutants produce defective cotyledons, including fused cotyledons, monocotyledons, multiple cotyledons, cup-shaped cotyledons and *mp*-like phenotype without hypocotyl with rudimentary root and a cotyledon-like structure with low penetrance (Chandler et

al., 2007). *ESR1* overexpression mutants have enlarged SAM, arrested vegetative meristem and radialized leaves (Kirch et al., 2003).

In case of *esr1-1 esr2-1* double mutant almost all of them manifested embryonic cell patterning defects and similar cotyledon phenotypes, including *mp*-like phenotype with increased penetrance. Whereas *esr1-1 esr2-2* double mutants are sterile, they form *pin*-like embryos without cotyledons and directly produce true leaves from SAM (Chandler et al., 2007).

Due to this similarity with auxin-signaling mutants was auxin speculated to mediate *ESR1* and 2 functions in non-cell-autonomous manner. This was then proved by analyzing *DR5* and *PIN1* expression in wild type and mutant background. Whilst in the wild type plants was *DR5* expressed in hypophysis and upper suspensor cell at 32-cell stage and at the base of the embryo and L1 layer at the tips of developing cotyledons. In *esr1-1* mutants was *DR5* expression diffusely centralized with asymmetrical maximum in basal domain at 32-cell stage and absence of *DR5* expression in abnormal cotyledons at heart stage was observed. *PIN1* expression in wild-type embryo was restricted to basal area, in *esr1* mutant it was localized in the center with lateral shift at 32-cell stage. This indicates that *ESR* acts upstream of auxin transport in embryonal development (Chandler et al., 2007). However MP was shown to promote transcriptional activity of *ESR1* promoter at the tips of embryonic cotyledons, placing *MP* upstream of *ESR1* expression, possibly acting in a feedback loop (Cole et al., 2009).

2.6.2 Link between *ESR* and *HD-ZIP III* genes

It has been also shown that *PHV* is spatio-temporally co-expressed with both *ESR* genes in proembryo and before being localized on the adaxial side of developing cotyledons is expressed in the apical portion of globular embryo. All *HD-ZIP III* members have similar expression pattern with *ESR* genes except for *ATHB8* (Emery et al., 2003). Moreover, the interaction between AP2 domain of both *ESR* proteins and PAS-like domain in MEKHLA domain of *PHV* have been demonstrated *in vitro* and *in vivo*. The same interaction has been confirmed for the rest of *HD-ZIP III* proteins (Chandler et al., 2007).

2.7 Formation of axillary and floral meristems

Plants form additional SAMs during post embryonic development which then leads to branching. These SAMs develop in junctions of leaves and stems, termed axils, therefore

called axillary meristems (AMs). AMs form first in the axils of the oldest leaves (Grbić and Bleecker, 1996). It has been proven that the AM and subtending leaf, termed bract, are related clonally (Irish and Sussex, 1992). AMs emerge on the adaxial side of the subtending leaf base (Talbert et al., 1995). This is supported by the emergence of axillary meristems from the down side of the leaves in *phb* mutant with adaxialized leaves (McConnell and Barton, 1998). *PINHEAD (PNH)* gene is expressed in adaxial portion of the leaf primordia and in SAM, presumably giving the adaxial leaf domain the competence to form meristems. Floral meristems on the other hand in most of the members of the *Brassicaceae* family form without apparent subtending bract. (Long and Barton, 2000).

The *STM* gene is expressed in all types of SAMs including floral meristems (FM) and AMs, and *STM* expression disappears in leaf primordia. Therefore, *STM* could be used as a marker of SAM fate. Leaf primordia are formed of cells pushed to the peripheral zone. In this zone there are cells expressing *STM* and cells lacking *STM* expression at positions predetermined for new leaves. The outline between cells expressing *STM* and *STM*-nonexpressing cells in leaves primordia become more discrete and linear as primordia get older (Long and Barton, 2000). A weak *stm-bum1* allele mutant plants form a partially functional SAM and are able to grow leaves (Jasinski et al., 2005). These mutants produce reduced number of axillary buds, mostly in rosette leaves. The cells in the axils are enlarged, indicating their differentiation. It was then proved that *STM* expression is required for AM initiation (Shi et al., 2016).

The axillary meristems arise from the axils of leaves in close association with the leaf base. *STM* is first expressed on the adaxial surface of the leaf primordia, then is restricted to the base of the axil. Later is the *STM* transcript located above leaf insertion point on its adaxial side before bud is formed. Axils with apparent bumps on the adaxial leaf base strongly express *STM* with no regions without *STM* expression. After this stage regions not expressing *STM* appear, indicating leaf primordia formation (Long and Barton, 2000). This pattern is observed in vegetatively growing *Arabidopsis* plants, where AMs form in older leaves before younger ones. Nonetheless after the stimulus inducing flowering this changes and the youngest leaves, termed cauline leaves, are the first to develop AMs (Hempel et al., 1998). The AMs emerge from undeveloped cauline leaves in contrast to AMs arising from rosette leaves, which are at the time fully developed (Long and Barton, 2000).

In order for AM to initiate auxin minimum and a pulse of cytokinin signaling is required (Y. Wang et al., 2014). *STM* expression was analyzed in plants ectopically accumulating auxin in leaf axils (Shi et al., 2016). These plants exhibited deficiency in AM initiation (Q. Wang et al., 2014). The *STM* expression was not detected in axils, while the cells were enlarged, presumably differentiated. Moreover it was shown that the auxin minimum is required for maintenance of low levels of *STM* transcripts, required for axillary bud formation (Shi et al., 2016). In the *rev-6* mutant that doesn't form AMs is maintained the expression of *STM* but does not increase during leaf maturation, indicating that REV is required for *STM* up-regulation necessary for AM initiation (Otsuga et al., 2001; Shi et al., 2016). The miRNA resistant overexpressing alleles of *HD-ZIPIII* genes were shown to promote ectopic AM formation in the abaxial leaf axils accompanied by *STM* up-regulation. In those leaf axils auxin minima required for the AM initiation were also measured (McConnell and Barton, 1998; Emery et al., 2003; Shi et al., 2016). The increase in *STM* expression can promote cytokinin biosynthesis (Jasinski et al., 2005). The cytokinin signaling pulse was proved to evoke *de novo* activation of *WUS* expression, crucial for AM initiation and its integrity (Wang et al., 2017).

ESR genes have been shown to be important for AM initiation (Tian et al., 2014). The *esr1* and *esr2* mutants have reduced number of AMs and undergo early flowering. The *esr1 rev-6* and *esr2 rev-6* double mutants manifest reduced axillary bud formation, when both *ESR* genes are mutated this phenotype is almost fully penetrant. Inducible expression of *REV* in *esr1 esr2* mutant background leads to slight increase in number of AMs of late rosette leaves, indicating the role of *ESRs* in AM initiation during early vegetative states (Zhang et al., 2018). The expression of *ESR* genes was located to leaf primordia, boundary cells and with strong expression in AMs. A reduction in level of *STM* was observed *esr* mutants, explaining the lack of AMs. *ESR 1* and *2* were then confirmed to up-regulate *STM*. (Zhang et al., 2018). Additionally, inducible overexpression of *STM* in *esr* mutants led to induction of axillary bud formation similarly as in *rev* mutant. The *STM* overexpression also partially rescued the phenotype of *esr1 esr2 rev-6* triple mutant (Shi et al., 2016; Zhang et al., 2018). *ESR1*, *ESR2* and *REV* were identified as activators of *STM* expression. They activate *STM* expression by binding to the same region in *STM* promoter (Shi et al., 2016; Zhang et al., 2018). Same as *ESR1/ESR2* physically interact with *REV* during embryogenesis, this interaction is crucial for the binding of either *ESR1* or *ESR2* to the *STM* promoter region (Chandler et

al., 2007; Zhang et al., 2018). The expression of *ZPR* genes, that inhibit the function of *REV*, is higher in young leaves and decreases in mature leaves prior to AM formation (Wenkel et al., 2007; Kim et al., 2008; Zhang et al., 2018). *ESR1/ESR2* compete with *ZPR3* for the interaction with *REV*. This suggests that *ZPR3* inhibits the activation of *STM* expression normally mediated by *ESR-REV* dimers (Zhang et al., 2018).

The FMs primordia develop from the flanks of inflorescence meristems (IMs). *STM* is negatively regulated on these flanks of the IM before floral primordium bulge appears. As the primordium grows *STM* expression spreads from IM into the primordium and the boundary between *STM* -expressing cells changes from convex to linear. With subsequent growth a sulcus appears between the IM and developing primordium. At this stage *STM* is expressed in the adaxial region of the primordia. At the positions of future sepal primordia, the *STM* expression is lost. Later sepal primordia become visible on the primordium (Smyth et al., 1990; Long and Barton, 2000). It was suggested that the FM emerges from an axil of a cryptic bract, that arises early in the development of floral primordium, marked by *STM*-negative region. This is consistent with the expression of *AINTEGUMENTA (ANT)* gene, which is expressed in organ primordia in the plant. The cryptic bract primordia expressed *ANT*, thus confirming this hypothesis (Long and Barton, 2000).

Two alternative models explaining AM formation have been proposed. The first: “detached meristem” model proposes that few pluripotent cells detach from primary SAM and become part of the axil as the leaf emerges from the SAM, supported by the presence of undifferentiated cells in the axils (McConnell and Barton, 1998; Long and Barton, 2000). The second model: “*de novo* induction” model proposing AM initiation from differentiated leaf cells (Long and Barton, 2000). This model was created following the observation of *phb-1d* mutant phenotypes, with axillary bud formation in the abaxial side (McConnell and Barton, 1998). A new “threshold model” was proposed showing that maintenance of low level of *STM* expression with subsequent increase in *STM* expression is required for AM initiation (Shi et al., 2016).

2.8 *WUSCHEL* independent SAM developmental pathway

wus loss-of-function mutant seedlings have the ability to form adventitious shoots without functional meristem. The shoots emerge between cotyledons and produce several leaves. Occasionally *wus* mutants can produce a flower primordium without meristematic

activity (Laux et al., 1996). *WUS* together with *STM* was identified as key players in regulation of SAM development (Gallois et al., 2002; Lenhard et al., 2002). However, *WUS* expression in the IM is low when compared to other types of SAMs and in *clv* enlarged SAMs the *WUS* expression is absent, showing that stem cells can be maintained without *WUS* (Schoof et al., 2000; Green et al., 2005).

An *ARGONAUTE10* (*AGO10*) gene, also known as PINHEAD (McConnell and Barton, 1995) /ZWILLE (Moussian et al., 1998) , is required for efficient SAM formation in embryogenesis and for axillary meristem formation (Lynn et al., 1999). *AGO10* prevents miR165/166 from repressing their targets (Liu et al., 2009; Ji et al., 2011). Since miR165/166 target HD-ZIP III members, the *ago10* mutants have reduced expression of all *HD-ZIP III* genes (Prigge et al., 2005) .

The *clv3 phb phv cna* quadruple mutant enhances the *clv3* phenotype, with large meristems, high number of stem cells and sterile flowers. However, *clv3* and also *clv3 phb phv cna* meristems have abnormal layering of the SAM, which isn't manifested in *phb phv cna* triple mutant (Lee and Clark, 2015). Whilst *wus* mutants can't form meristems, the *wus phb phv cna* quadruple mutants can produce up to 8 leaves before termination of the SAM. After the termination the quadruple mutants produce several adventitious meristems capable of forming leaves and inflorescences, occasionally fasciated. The quadruple mutants have a SAM-like structures, similar to wild type SAM, but less defined. *wus* is then expressed in the apical region of the seedling and in axils of cotyledons and leaves, corresponding to the positions of SAM-like structures. The suppression of *wus* phenotype by *phb phv cna* is exclusive to vegetative and early reproductive stage. In order to suppress *wus* phenotype all PHB, PHV and CNA must be inactive. The role of PHB/PHV/CNA is then to limit stem cell population in CLV/WUS parallel pathway (Lee and Clark, 2015).

3 Material and methods

3.1 Material

3.1.1 Plant material

As control plant and for introgression from Landsberg erecta (Ler) and Enkheim (En-2) ecotypes, was used the Columbia (Col-0) ecotype. Single mutants are Col-0 ecotype if not stated different.

For the experiments were used the following mutants:

- *wus-101* – T-DNA insertion in 1st exon; GK-870H12
- *esr1-1* – double stranded transposon in exon; N121728
- *esr1-2* – T-DNA insertion 7 bp upstream of stop codon; N321463
- *esr2-2* – 2bp deletion creating premature stop codon; 6AVB35
- *athb8* – T-DNA insertion in second exon; SALK_065586
- *cna-2* – T-DNA insertion in last exon; N513142
- *icu4-1d* – G to A transition in miRNA complementary sequence; En-2 ecotype; obtained from Micol, Spain
- *phb* – T-DNA insertion in exon; SALK_008924C
- *phv* – T-DNA insertion in 1st exon; SALK_899C08
- *phv-1d* – G to A transition in miRNA complementary sequence; Ler ecotype; N65908
- *rev-5* – EMS knock-out; A260V
- *revG581E* – Tilling in Col-0 *er-105* (erecta mutation) background; N90262
- *se-2* – T-DNA insertion in 10th exon; SAIL_44_G12

3.1.2 Chemicals

- Acetic acid (Sigma Aldrich)
- Agarose (Sigma Aldrich)
- Basta (BASF)
- dNTP mixture 10 mmol·L⁻¹(Promega)
- ddH₂O (Sigma Aldrich)
- EDTA (Sigma Aldrich)
- Ethanol 96% (V/V) (Penta)

- Ethidium bromide (NeoLab)
- Chloroform: Isoamyl alcohol 24:1 (CIA; Sigma Aldrich)
- Gellan gum (Sigma Aldrich)
- GeneRuler™ 1 kb Plus DNA Ladder (Thermo-Scientific)
- Kanamycin (Kan; Sigma Aldrich)
- Magnesium chloride 25 mmol·L⁻¹ (MgCl₂; Promega)
- MES (2-(N-morpholino) ethane sulfonic acid; Sigma Aldrich)
- Murashige&Skoog basal salt mixture with vitamins (MS salt; Sigma Aldrich)
- Plant agar (Thomas Scientific)
- Potassium hydroxide (KOH; Sigma Aldrich)
- Sodium chloride (NaCl; Sigma Aldrich)
- Sodium dodecyl sulfate (SDS; Sigma Aldrich)
- Sodium hypochlorite (NaOCl; VWR Chemicals)
- Sucrose (Sigma Aldrich)
- Sulfonamide (Sigma Aldrich)
- Tris-HCl (pH 8; Sigma Aldrich)
- 5x GoTaq® Flexi Buffer (Promega)
- 5x GoTaq® Flexi Green Buffer (Promega)

3.1.3 Solutions and culture media

Genomic DNA extraction buffer:

- 200 mmol·L⁻¹ Tris-HCl pH 8
- 250 mmol·L⁻¹ NaCl
- 20 mmol·L⁻¹ EDTA
- 0,5 % SDS

½ Murashige&Skoog (MS) media (1 L):

- 4,3 g MS salt
- 10 g Sucrose
- 0,5 g MES
- 6 g Gellan gum (or 10 g Plant agar in medium with Kan)
- Add ddH₂O to 1 L and adjust with KOH to pH 5,7 before addition of gellan gum

- Antibiotics: Kan 25 mg/L (final concentration)
Sulf 2 mg/L (final concentration)

Sterilization solution (20 mL):

- 10 mL 50% NaOCl
- 2 mL 70% Ethanol
- 8mL ddH₂O

1x TAE buffer:

- 40 mmol·L⁻¹ Tris-HCl pH 8
- 20 mmol·L⁻¹ Acetic acid
- 1 mmol·L⁻¹ EDTA

TE buffer:

- 10 mmol·L⁻¹ Tris-HCl pH 8
- 1 mmol·L⁻¹ EDTA

3.1.4 Enzymes

- GoTaq Flexi DNA polymerase – 5 000 U·mL⁻¹ (Promega)
- BamHI – 20 000 U·mL⁻¹ (NEB, USA)
- EcoRI – 20 000 U·mL⁻¹ (NEB, USA)
- EcoRV – 20 000 U·mL⁻¹ (NEB, USA)
- SnaBI – 20 000 U·mL⁻¹ (NEB, USA)

3.1.5 Laboratory equipment and devices

- Analytical balance 5034/120 (Auxilab)
- Appliances for agarose electrophoresis
- Autoclave HST 5-6-8 (Zirbus)
- Automatic pipettes with tips (Eppendorf)
- Axio Zoom.V16 microscope (ZEISS)
- Cooled centrifuge 5417R (Eppendorf)
- Digital camera OM-D E-M5 Mark II (Olympus)
- Flowbox (MERCİ)
- Forceps

- Gel Doc EZ Gel Documentation System (BioRad)
- Incubator (25 °C) (Lovibond)
- Laboratory glassware
- Magnetic stirrer RH basic 2 IKAMAG (IKA)
- Microtubes (1,5 mL; 2 mL), Safe-lock microcentrifuge tubes (1,5 mL) (Eppendorf)
- PCR strips (ThermoFisher Scientific)
- Petri dishes
- pH meter (Eutech Instruments)
- Stereoscopic Zoom Microscope SMZ1000/SMZ800 (Nikon)
- Thermocycler Applied Biosystems Veriti (Life Technologies)
- TissueLyser II with adapters (Qiagen)
- Tungsten Carbide Beads, 3 mm (Qiagen)
- Vacuum controller (KNF Neuberger)
- Vortex (Labnet)

3.1.6 Software

- GIMP
- ImageJ
- Image lab (Bio-Rad)
- MS Office Excel 365
- ZEN Blue 2012 (ZEISS)

3.1.7 Primers

All primers were designed and ordered from Sigma-Aldrich. The primer sequences used are listed in Table 1.

3.2 Methods

3.2.1 ½ MS solid medium preparation

The prepared ½ MS medium in 1 L bottle was sterilized in autoclave (30 minutes, 121 °C, 15 psi pressure). After sterilization the antibiotics were added if needed and the medium was then poured into Petri dishes (20 – 25 mL per dish).

Table 1 List of used primers for PCR genotyping

Allele	Primer	Sequence
<i>athb8</i>	Forward	CTCCAACATCGAGCCTAAACAG
	Reverse	GCGCCAAGAGTTATAAACCTAG
	T-DNA	GGTTCACGTAGTGGGCCATCGCCCTG
<i>cna-2</i>	Forward	GCTGAGGAGTAATGGCAATGTCTTG
	Reverse	AAAGAACCAACCCTGCAGGACTAGC
	T-DNA	TAACGCTGCGGACATCTACATTTTTG
<i>esr1-1</i>	Forward	GTGCAACTCAAAGTTTCCATGC
	Reverse	AAAATTAGTACGAGCCTTTGCTC
	Transposon	GTTTTGGCCGACACTCCTTACC
<i>esr1-2</i>	Forward	GCTCCATCTCTTTCAAACATCAACCA
	T-DNA	GGGCTACACTGAATTGGTAGCTC
<i>esr2-2</i>	Forward	CCGTTAACCCTTTCGCTTACCCGCCTTGAT
	Reverse	GGTACTTGACCTCTTAGCTTTAGGCGA
<i>icu4-1d</i>	Forward	GGTTGTTTTTGTATTTTCCGTAACAGCCGG
	Reverse	GCACCCTTGTAGGCTCAAGACC
<i>phb</i>	Forward	CCTTCTTCAAACCTTTGTGAGAGC
	Reverse	AGAGAGGCCTCATGACTTCAGG
	T-DNA	CTGAATTTTCATAACCAATCTCGATACAC
<i>phv</i>	Forward	CCATGGACGATAGAGACTCTCC
	Reverse	GTTGTCTTCTCAGAGAGCTAGG
	T-DNA	CTGAATTTTCATAACCAATCTCGATACAC
<i>rev-5</i>	Forward	TAAAGTTGTGACATTTGTTTCAGACGTACG
	Reverse	AGGCTCGTTGTGTATCTCAGG
<i>rev-G581E</i>	Forward	ATCCGGTTCCTTAGAGAGCATC
	Reverse	AGAATACATCTCGAGCTTGAGC
<i>wus-101</i>	Forward	CACGGTGTCCCATGCAGAGACC
	Reverse	TCACCGTTATTGAAGCTGGGATATGG
	T-DNA	GGGCTACACTGAATTGGTAGCTC

3.2.2 Seed sterilization

Small amount of seeds was transferred into 1,5 mL microtube (approximately 50-100 seeds). Then 800 μ L of 70% ethanol was added to the tube and the seeds were incubated for 2-3 minutes. After removal of ethanol 1 μ L of sterilization solution was added and the seeds were incubated for 10-12 minutes while occasionally shaking the tube. After removing the solution were the seeds washed three times with ddH₂O. After washing were the seeds either sewed on the media or 200 μ L of ddH₂O was added to the tube. Seeds on media or in tube were then transferred to fridge (4°C) for 24 hours and passed the stratification phase. The whole process is performed in sterile conditions.

3.2.3 Plant growing

The plants were grown at following conditions: photoperiod 16 h light and 8 h dark, light intensity $130 \mu\text{mol}\cdot\text{m}^{-2}\cdot\text{s}^{-1}$, humidity 65 % and temperature 25 °C.

Seedlings grew either on media in Petri dishes, enriched with Kan for *cna-2* and with Sulf for *wus-101* and *esr1-2* T-DNAs selection, or were sewn directly to the soil. Seeds of *se-2* were sewn on soil and sprayed with Basta solution. Seedlings growing in Petri dishes were transferred to the soil 7th day post germination.

3.2.4 Genomic DNA extraction

Small true leaf (3x3 mm) of *Arabidopsis* seedling was transferred into 1,5 mL safe-lock tube along with a tungsten bead. Then 300 μL of extraction buffer and 70 μL of CIA was added. Prepared set of tubes was placed into TissueLyser adapters and the adapters were stabilized in the TissueLyser. The leaves were then lyzed for 2 minutes with set frequency to 25 Hz. The tubes with lyzed leaves were transferred into pre-cooled (8°C) centrifuge and centrifuged for 3 minutes at 14 000 rpm.

After centrifugation was the supernatant containing genomic DNA transferred into 1,5 mL microtube. 700 μL of 96% ethanol was then added and tubes are transferred into the centrifuge where they were kept for approximately 10 minutes before they were centrifuged for 10 minutes at 14 000 rpm.

All liquid was removed from the tube after centrifugation and 75 μL of 70% ethanol is added to wash the precipitated DNA on the wall of the tube. Then the samples are once more centrifugated at 14 000 rpm for 3 minutes and when the centrifugation is finished all liquid is removed. To the precipitate was added 50 μL of TE buffer and the precipitated DNA was dissolved into the buffer by using vortex. The DNA prepared solution was stored at -20 °C until genotyping.

3.2.5 PCR genotyping

During the preparation of PCR samples, we worked on ice to prevent DNA denaturation and enzyme degradation.

First the master mix was prepared into 2 mL microtube. For one sample the volumes are the following:

- 3,4 μL ddH₂O

- 2 μL 5x GoTaq® Flexi Green Buffer
- 1 μL MgCl_2 25 $\text{mmol}\cdot\text{L}^{-1}$
- 1 μL dNTP mixture 10 $\text{mmol}\cdot\text{L}^{-1}$
- 0,8 μL forward primer
- 0,8 μL reverse primer
- 0,05 μL GoTaq Flexi DNA polymerase – 5 000 $\text{U}\cdot\text{mL}^{-1}$

If three primers are used, then the volume of ddH₂O is reduced by the same volume as the volume of the third primer (0,8 μL) to keep the same reaction volume.

Total volume of 9 μL was pipetted into one PCR strip compartment per each sample. Then 1 μL of DNA solution was added and both solutions were mixed by pipetting. PCR strips were transferred into thermo cycler to convey the PCR. The conditions of PCR are listed in Table 2.

3.2.6 DNA electrophoresis

Firstly, the agarose gel was prepared. The concentration of gels varied between 1,7 to 3,0 % (w/v) depending on the PCR/restriction product size (the smaller the product the denser the gel). The amount of agarose was mixed with needed volume of 1x TAE buffer and ethidium bromide is added to final concentration of 0,5 $\mu\text{g}/\text{mL}$. The mixture was heated in microwave oven and homogenized.

The liquid agarose gel was the poured into electrophoretic gel tray and bubbles were removed. The gel then solidifies for approximately 15 minutes at horizontal position. The solid gel was then placed into an electrophoretic chamber and covered with 1x TAE buffer. Into each well was added 7 μL of PCR/restriction product and 2 μL of DNA ladder was added into each tenth well. The PCR/restriction products were then separated at voltage of 120 V for 12 minutes. The gel was then scanned by the Gel DocTM EZ Imager and analyzed in Image LabTM software.

Table 2 PCR conditions.

Step	Temperature	Time	Number of cycles
initiation	95 °C	1 min	1
denaturation	95 °C	20 s	
annealing	57 °C	20 s	32
extension	72 °C	20 s	
final extension	72 °C	4 min	1

3.2.7 DNA restriction

PCR products of *esr2-2*, *icu1-4d*, *rev-5* and *revG581E* were restricted by restriction endonucleases EcoRV, BamHI, SnaBI and EcoRI respectively. *esr2-2*, *icu4-1d* and *revG581E* mutations are CAPS (Cleaved amplified polymorphic sequence) markers and form a restriction site. Restriction site in *rev-5* is a dCAPS (Derived Cleaved Amplified Polymorphic Sequence) marker and is created by primer mismatch. A master mix was prepared in 2 mL microtube with following volumes for each PCR product:

- 3 µL ddH₂O
- 0,8 µL 5x GoTaq® Flexi Buffer
- 0,2 µL restriction enzyme

1,3 µL of master mix was pipetted to a PCR strip compartment and 2,5 µL of PCR product was added. Prepared samples were placed into an incubator with temperature set to 30 °C for 6 h. The restriction products were then analyzed by electrophoresis.

3.2.8 Plant crossing

From the inflorescences of mother plant were removed the mature siliques. The immature anthers of inflorescence buds were removed with forceps. The inflorescence was then marked by a piece of red tape. After 3 days an anther filament from mature flower of father plant was applied to the stigma of marked inflorescence by forceps to cover it with pollen.

In order to make higher order mutants, *athb8*, *cna-2*, *esr1-1*, *esr1-2*, *esr2-2*, *phv*, *phb*, *rev-5* and *wus-101* were backcrossed at least 4 times and *revG581E* was backcrossed 3 times at the time of our experiments. *icu4-1d* and *phv-1d* were introgressed into Col-0 by repetitive crossing with Col-0 plants six times.

esr1-1 esr2-2 mutant, which produces viable seeds, was made. By crossing it with *wus-101* /+ was obtained *wus-101 esr1-1 esr2-2* triple mutant. *wus-101* /+ was also crossed with *esr1-1*, *esr1-2*, *phb*, *phv*, *rev-5* and with *rev-5 esr1-1*, *rev-5 esr2-2* in order to obtain *wus-101 esr1-1*, *wus-101 esr1-2*, *wus-101 phb*, *wus-101 phv*, *wus-101 rev-5* double mutants and *wus-101 rev-5 esr1-1*, *wus-101 rev-5 esr2-2* triple mutants. Finally a *phb phv cna-2* triple mutant was crossed with *wus-101* /+ and the obtained *wus-101 phb phv cna-2* quadruple mutant was crossed with *esr1-1* and *esr1-1 esr2-2* to create *wus-101*

phb phv cna-2 esr1-1 quintuple and *wus-101 phb phv cna-2 esr1-1 esr2-2* sextuple mutants.

Additionally, *rev-5* mutant was crossed with *athb8*, *cna-2*, *phb*, *phv* and *esr1-1 esr2-2*. *rev-5 athb8*, *rev-5 cna-2*, *rev-5 phb*, *rev-5 phv* double mutants and *rev-5 esr1-1 esr2-2* triple mutant were obtained.

3.2.9 Phenotypical analysis

7 to 10 days old mutant seedlings were observed by stereomicroscope and their above ground organ phenotypes were compared to Col-0.

Lateral meristems of 30 days old *icu4-1d*, *phv-1d*, *rev-5*, *revG581E*, *rev-5 athb8*, *rev-5 cna-2*, *rev-5 phv*, *rev-5 phb*, *rev-5 esr1-1 esr2-2* and 50 days old *se-2* plants was analyzed. We analyzed lateral organ phenotypes shown in figure 5.

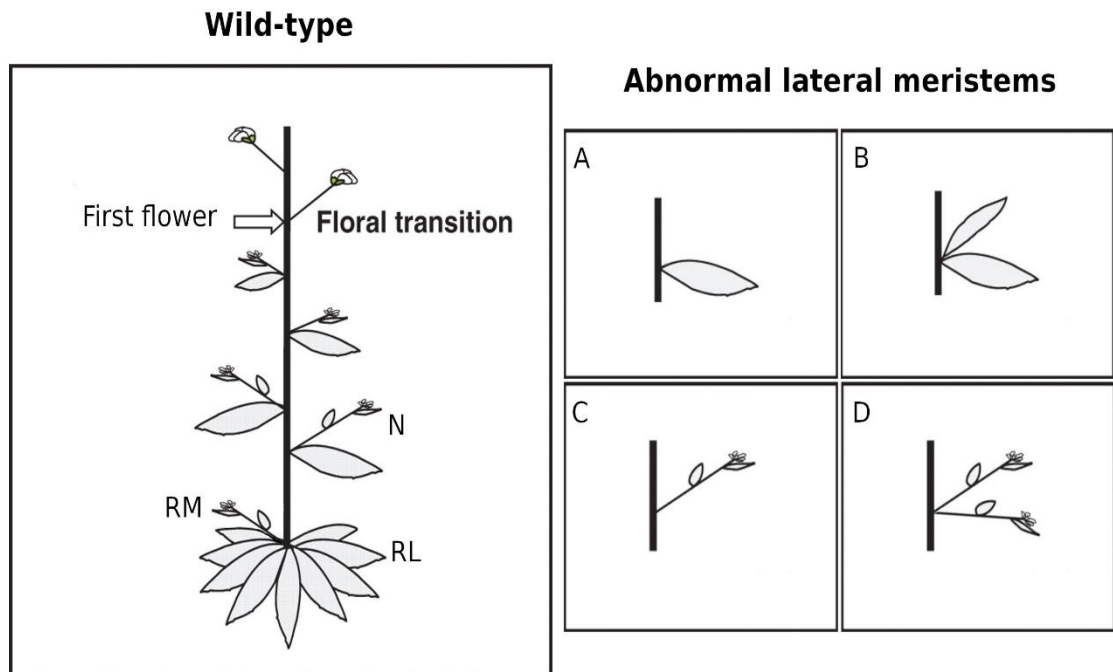


Figure 5 Lateral organ phenotypes in wil-type (left) and abnormal phenotypes in mutant plants (right). RL - rosette leaf, RM- meristem from rosette leaf axil, N - normal paraclade+bract structure, A - bract only, B - paraclade replaced with cauline leaf, C - paraclade without bract, D - bract replaced with paraclade. Adapted from (Pouteau and Albertini, 2011) and edited.

4 Results

In this work we focused on the interactions between *ESR* genes and *HD-ZIPIII* genes (Chandler et al., 2007) that were manifested phenotypically. Moreover, we observed these interactions in *wus-101* background as the *WUS*-independent pathway of SAM development have been described earlier (Lee and Clark, 2015).

4.1 Seedling phenotype analysis

At 8th day post germination wild-type seedling have formed two pairs of true leaves (Figure 6A). The *wus-101* seedling at this time formed only one true leaf (Figure 6B). When *esr1-1* mutation was added to *wus-101*, no signs of meristematic activity were observed (Figure 6C). Introduction of both *esr1-1* and *esr2-2* into *wus-101* led to pleiomorphic phenotypes, indicating a developmental dysfunction of the SAM and of the

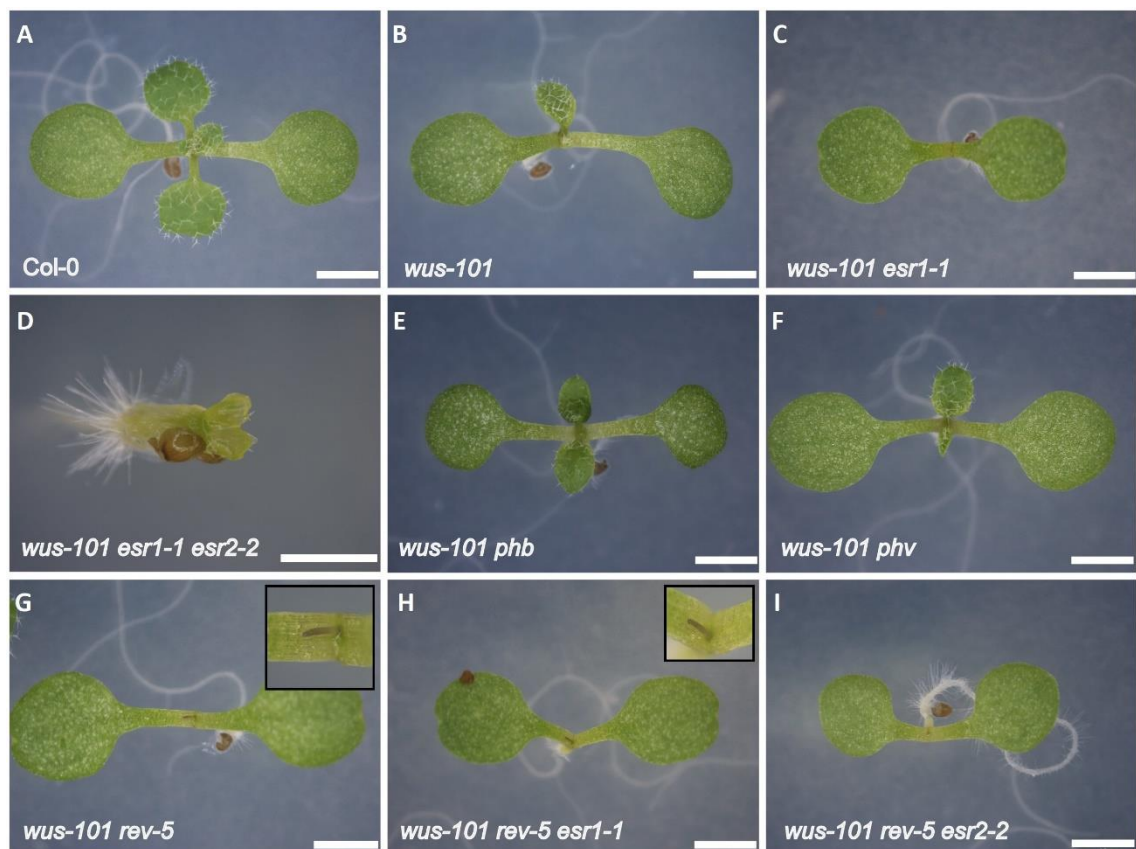


Figure 6 Lateral organ development in *WUS*-independent pathway of 8 days old seedlings. (A) Col-0, (B) *wus-101* with one true leaf, (C) *wus-101 esr1-1* without meristematic activity, (D) *wus-101 esr1-1 esr2-2* malformed seedling, (E) *wus-101 phb*, (F) *wus-101 phv*, (G) *wus-101 rev-5* with pin-like structure, (H) *wus-101 rev-5 esr1-1* with radialized pin-like structure, (I) *wus-101 rev-5 esr2-2* without signs of meristematic activity. Scale bars = 1 mm (D), 2 mm for the rest.

root (Figure 6D). Both *wus-101 phb* and *wus-101 phv* produced one pair of true narrow leaves (Figure 6E, F). Interestingly the *wus-101 rev-5* double mutant didn't form any true leaves and formed a pin-like radialized structure between cotyledons. The same phenotype was observed in *wus-101 rev-5 esr1-1* triple mutant (Figure 6G, H). This indicates that *rev-5* might play a key role in manifestation of this phenotype. However, the *wus-101 rev-5 esr2-2* triple mutant showed no signs of meristematic activities (Figure 6I) similarly to *wus-101 esr1-1*.

We analyzed another set of seedlings at 7 days post germination (Figure 7). While the wild-type had already formed one pair of true leaves and another was emerging (Figure 7A) the *wus-101* showed emergence of one pair of true leaves (Figure 7B). The *esr1-1 esr2-2* double mutant showed no signs of meristematic activity (Figure 7C, D) and occasionally had partially fused cotyledons (Figure 7C). The *wus-101 esr1-2* double mutant, where *esr1-2* is the weaker allele of *esr1*, formed a radialized structure between cotyledons (Figure 7E) but also a phenotype with one true leaf was observed (Figure 7F). The *wus-101 rev-5* seedlings formed a pin-like radialized structure (Figure 7G) same as in previous observation. Although, in this observation the *wus-101 rev-5 esr1-1* triple mutant exhibited a pleiomorphic phenotype, showing a pin-like structure (Figure 7L), lacking visible meristematic activity (Figure 7H) or cotyledonary fusion with a cup-shaped true leaf (Figure 7I). The *wus-101 phb phv cna (wus-101 ppc)* quadruple mutant was able to form true leaves similarly to the wild-type, but the leaves were smaller (Figure 7J). We also observed what seemed to be triple cotyledon with two cotyledons fused (Figure 7K). However, this confirms that the *phb phv cna-2* triple mutation suppresses the *wus-101* phenotype. The *wus-101 esr1-1 phb phv cna-2 (wus-101 esr1-1 ppc)* quintuple mutant shows also pleiomorphic phenotypes. They form true leaves, but the leaves are often radialized (Figure 7M, O). Also, cotyledon phenotypes were observed, ranging from asymmetrically placed cotyledons (Figure 7O), through cotyledon malformation (Figure 7N) and absence of one cotyledon (Figure 7N, P), to complete absence of cotyledons (Figure 7Q). In few seedlings we observed severe defects in development, including root development, but we were still able to observe leaf-like structures (Figure 7Q, R). The *wus-101 esr1-1 esr2-2 phb phv cna-2 (wus-101 esr1-1 esr2-2 ppc)* show even stronger defects, having arrested meristem development (Figure 7S, T). This indicates that *ESR1* and *ESR2* have redundant function and are necessary for establishment of lateral organs through *WUS*-independent pathway.

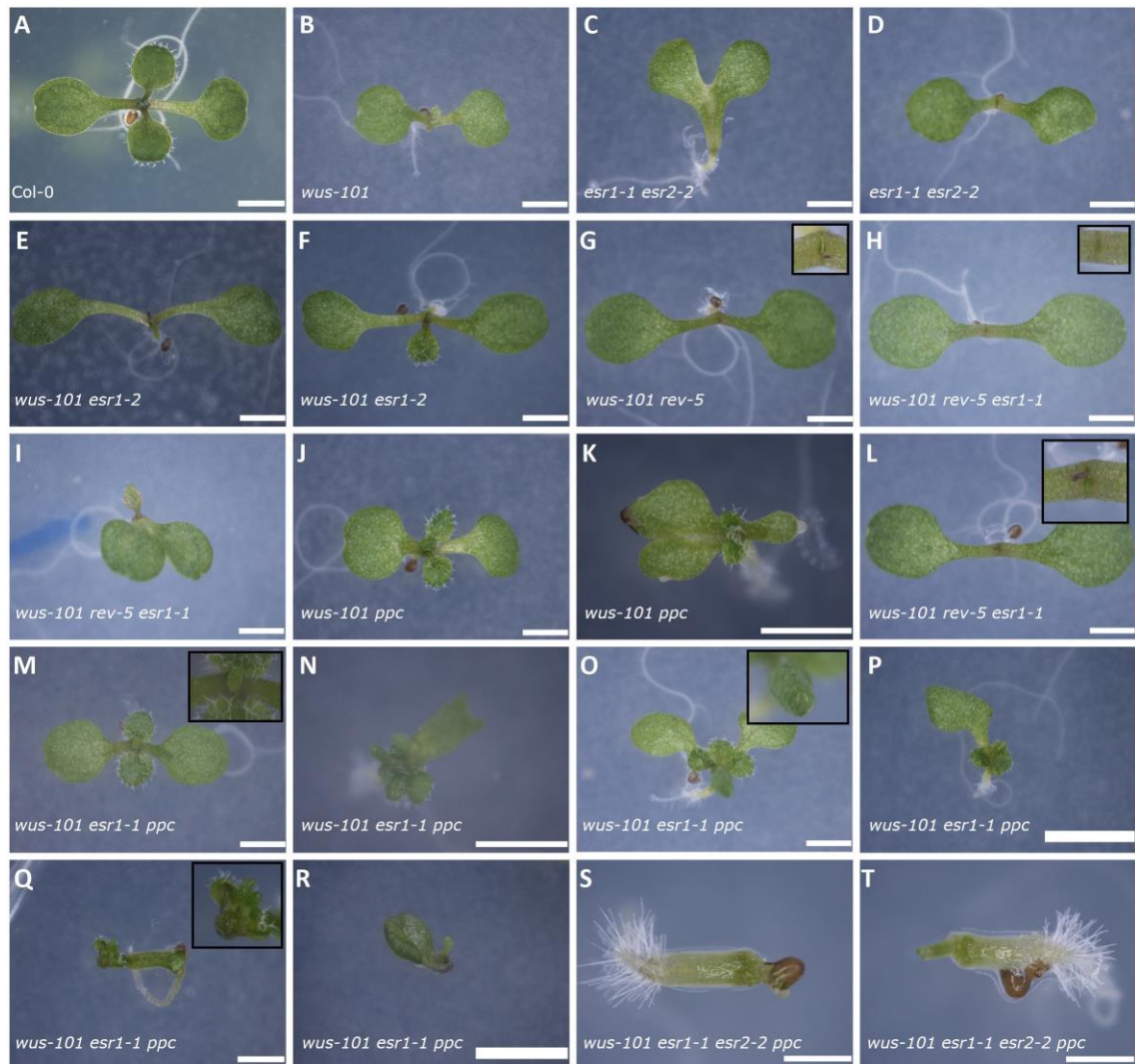


Figure 7 *WUS*-independent pathway of later organ formation in 7 days old seedlings. (A) Col-0, (B) *wus-101* with small true leaves, (C, D) *esr1-1 esr2-2* showing no signs of meristematic activity, (E) *wus-101 esr1-2* with radialized structure, (F) *wus-101 esr1-2* with one true leaf, (G) *wus-101 rev-5* with radialized structure, (H, I, L) *wus rev-5 esr1-1* without pin-like structure, with fused cotyledons and cup-like true leaf and with radialized pin-like structure respectively, (J, K) *wus-101 phb phv cna-2* forming true leaves and in (K) showing 3 cotyledons with 2 of them fused, (M-R) *wus-101 esr1-1 phb phv cna-2* forming true leaves, often radialized (M-O, R), exhibiting cotyledonary defects (N-R) and root defects (Q, R), (S, T) *wus-101 esr1-1 esr2-2 phb phv cna-2* showing severe developmental defects with small roots covered by root hairs, a mass of white to green tissue ending with a thin structure. Scale bars = 2 mm (A-R), 1 mm (S, T).

We then focused on the *wus-101 esr1-1 esr2-2 phb phv cna-2* sextuple mutant seedlings. 10 days old seedlings of *wus-101/+ esr1-1 esr2-2 phb phv cna-2* self-progeny, selected on Sulf, were screened by the Axio Zoom microscope. We observed defects in leaf formation, for example single true leaf emerging from the SAM with additional thin structures, which could be radialized leaves (Figure 8D). In one plant we observed absence of true leaves, four cotyledons and duplicated meristem-like structures (Figure

8E). These meristem-like structures have a bulge of light green tissue in the middle and are surrounded by a dark green tissue (Figure 8E, F). Single cotyledonous small seedling with multiple small and round leaves was also observed (Figure 8C). In some plants a radialized structure was observed emerging in between the cotyledons (Figure 8G). Several seedlings were malformed, with a mass of green to white tissue, having a small root covered in root hair (Figure H, I). In comparison *wus-101 esr1-1 phb phv cna-1* produced many unorganized narrow leaves but has also formed a radialized structure (Figure 8B). The number of leaves was higher than number of true leaves in wild type plant (Figure 8A).



Figure 8 Development of lateral organs in 10 days old *wus-101 esr1-1 esr2-2 phv phb cna-2* seedlings. (A) wild-type, (B) *wus-101 esr1-1 phv phb cna-2*, note the radialized structure, (C-I) *wus-101 esr1-1 esr2-2 phv phb cna-2*. (C) Single cotyledon and leaf number comparable to wild-type, but with no obvious stem and smaller in size, (D) single true leaf with additional narrow thin structures (arrow), (E) seedling with four cotyledons, double meristem-like structure with a bulging tissue in the middle and one narrow leaf-like structure (arrow), (F) meristem-like structure with mass of tissue, (G) a radialized structure emerging between cotyledons, (H) green mass of tissue with a white tip having root hairs on the base (top), (I) white mass of tissue passing to root tissue with root hairs. Scale bars = 2 mm (A,B, D, E), 1mm (C), 0,5 mm (F, G), 0,2 mm (H, I).

These data indicate that the *ESR1* and *ESR2* are required for the *WUS*-independent SAM developmental pathway. This pathway is observed in the *wus-101 phb phv cna-2* mutant, which somehow rescues the *wus-101* phenotype (Lee and Clark, 2015).

4.2 Phenotype analysis of mature plants

4.2.1 Lateral organ development

We analyzed phenotypes of lateral organ formation in plants 30 days after germination *rev-5*, *revG581E*, *rev-5 atb8*, *rev-5 cna-2*, *rev phb*, *rev phv* mutants, because it has been previously described that *rev* mutants form less lateral and floral meristems (Otsuga et al., 2001). The *rev-5 phb* and *rev-5 esr1-1 esr2-2* were self-progeny of *rev-5 phb/+* and *rev-5 esr1-1 esr2-2/+* respectively, because they can't be otherwise maintained. We then compared these with *icul-4d* (gain-of-function for *CNA*) and *phv-1d* (*PHV* gain-of-function). We also analyzed 50 days old *se-2*, lacking functional miR165/166 and thus resulting in similar phenotypes to HD-ZIPIII gain-of-function mutants. We analyzed the phenotypes shown in Figure 5, namely: rosette leaves (RL), meristems from rosette leaves axils (RM), normal paraclade subtended by a bract (N), bract only, without paraclade (A), paraclade replaced by a bract (B), paraclade without bract (C) and bract replaced by a paraclade (D).

The *rev* mutants didn't develop paraclades from cauline leaf axils significantly more often than wild-type plants and formed significantly less phenotypically normal lateral meristems (Table 3). The frequency of abnormalities was higher in *rev-5* mutant, showing that it's a stronger allele. The frequency of normal lateral meristem phenotype increased in *rev-5 cna-2* and *rev-5 atb8*, showing their antagonistic function. Interestingly in *rev-5 phb* double mutant all lateral meristems lacked a paraclade. In *rev-5 phv* this was slightly lower (91,58 %) but still much higher than in *rev* single mutants. This suggests that *phb* and *phv* play an agonistic function with *rev* in lateral organ development. This is supported by the lethal phenotype of *rev-5 phb phv* triple mutant. In the *rev-5 esr1-1 esr2-2* the frequency of missing paraclade significantly increased when compared to *rev* mutants (50 %) but was lower than in *rev-5 phb* and *rev-5 phv*.

When the gain-of-function mutants were analyzed we didn't observe significant difference when compared to Columbia, except for *phv-1d* where 18,46 % of lateral meristems were formed by two paraclades above each-other. This even strongly supports

Table 3 Lateral organ phenotypes frequencies. N=normal paraclade subtended by a bract, A=bract only, B=paraclade replaced by a bract, C=paraclade without bract, D=bract replaced by a paraclade.

Genotype	N (%)	A (%)	B (%)	C (%)	D (%)	n
Col-0	100,00	0,00	0,00	0,00	0,00	48
<i>rev-G581E</i>	85,12*	10,74*	3,31	0,83	0,00	56
<i>rev-5</i>	77,60*	16,00*	5,60	0,80	0,00	53
<i>cna-2 rev-5</i>	92,80	4,80	1,60	0,80	0,00	57
<i>athb8 rev-5</i>	88,00*	7,20	4,00	0,80	0,00	56
<i>phb rev-5</i>	0,00*	100,00*	0,00	0,00	0,00	77
<i>phv rev-5</i>	7,37*	91,58*	0,00	1,05	0,00	51
<i>esr1-1 esr2-2 rev-5</i>	50,00*	50,00*	0,00	0,00	0,00	56
<i>icu-4d</i>	95,54	0,64	0,00	0,64	3,18	50
<i>phv-1d</i>	75,38*	4,62	0,00	1,54	18,46*	48
<i>se-2</i> †	92,45‡	6,04§	0,00	1,51	0,00	72

* p < 0,05

† 50 days old plants

‡ 73,87 % with additional leaves

§ 88,89 % with visible bud in bract axil

the key role of *phv* in lateral organ development, namely paraclade, because in this mutant *PHV* is overexpressed. Notably most of *se-2* otherwise normal lateral organs had more than one cauline leaf (73.87 %), which after closer observation was described as early branching.

We then focused on the rosette leaves phenotypes and on the meristems from its axils. The *rev* mutants produced in average significantly less rosette leaves ($9,98 \pm 1,8$ for *rev-5* and $10,57 \pm 1,98$ for *revG581E* per plant) when compared to wild-type ($13,46 \pm 2,68$). With these correlates the mean number of axillary meristems from rosette leaves, which was also significantly reduced (Table 4). Mutations in *phb*, *phv* and both *esr1-1 esr2-2* added to *rev-5* mutation resulted in significant decrease in number of rosette leaves when compared to *rev-5* single mutant (p-values < 0,001) and interestingly the *rev-5 cna-2* double mutant formed less rosette leaves than *rev-5* mutant (p = 0,003). This contrasts with its phenotype of lateral organ development. However, the number of axillary meristems of rosette leaves was significantly lower only in *rev-5 phb*, *rev-5 phv* and *rev-5 esr1-1 esr2-2* when compared to *rev-5* (p-values < 0,001). More concretely the *rev-5 phb* and *rev-5 phv* didn't form any meristems from rosette leaves axils.

The *icu4-1d* and *phv-1d* both formed more rosette leaves than the wild-type but only *icu-4d* formed in average more axillary meristems than Col-0 (p < 0,001). In these gain-of-function mutants we focused more on the leaf phenotype. 95,14 % of *icu4-1d*

Table 4 Rosette leaves and meristems phenotypes. RL=rosette leaves, RM= meristem from rosette leaf axil

Genotype	RL	RM	upward-curved RLs (%)	cup-shaped RLs (%)	n
Col-0	13,46±2,68	2,65±0,95	0,00	0,00	48
<i>rev-G581E</i>	10,57±1,98*	0,73±0,81*	0,00	0,00	56
<i>rev-5</i>	9,98±1,80*	0,72±0,76*	0,00	0,00	53
<i>cna-2 rev-5</i>	9,02±1,41*	0,81±0,58*	0,00	0,00	57
<i>athb8 rev-5</i>	9,77±2,05*	0,63±0,61*	0,00	0,00	56
<i>phb rev-5</i>	8,87±1,11*	0,00*	0,00	0,00	77
<i>phv rev-5</i>	8,63±0,93*	0,00*	0,00	0,00	51
<i>esr1-1 esr2-2 rev-5</i>	7,64±1,98*	0,16±0,49*	0,00	0,00	56
<i>icu-4d</i>	11,12±2,43*	4,60±0,87*	95,14*	0,00	50
<i>phv-1d</i>	11,98±2,94*	3,02±0,97	17,74*	8,87*	48

* p < 0,05

rosette leaves were curved upward, showing role of *CNA* in leaf polarity. The *phv-1d* rosette leaves were only curved upward in 17,74 % but 8,87 % of rosette leaves were cup shaped (similar to Figure 7I). The *se-2* rosette leaf phenotype wasn't analyzed because of extensive branching and its age.

4.2.2 Inflorescence meristem development

We analyzed phenotypes of inflorescence meristems in *rev-5*, *revG581E*, *rev-5 athb8*, *rev-5 cna-2*, *rev phb*, *rev phv* mutants. While *rev-5* wasn't much different from the wild-type (Figure 10A, B) the *revG581E* formed smaller flower buds and smaller siliques, often with arrested development (Figure 10C). Compared to wild-type both *rev-5 athb8*

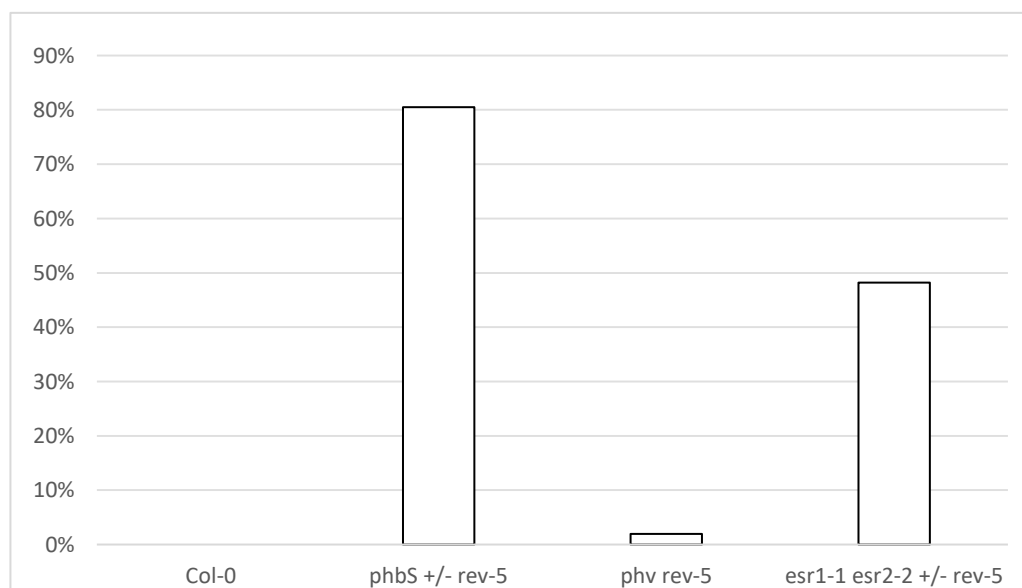


Figure 9 Frequency of pin-like apical structure.

and *rev-5 cna-2* seemed to produce more flowers (Figure 10D, E). The *rev-5 phv* double mutant often formed inflorescences of filamentous structure (Figure 10F). Similar

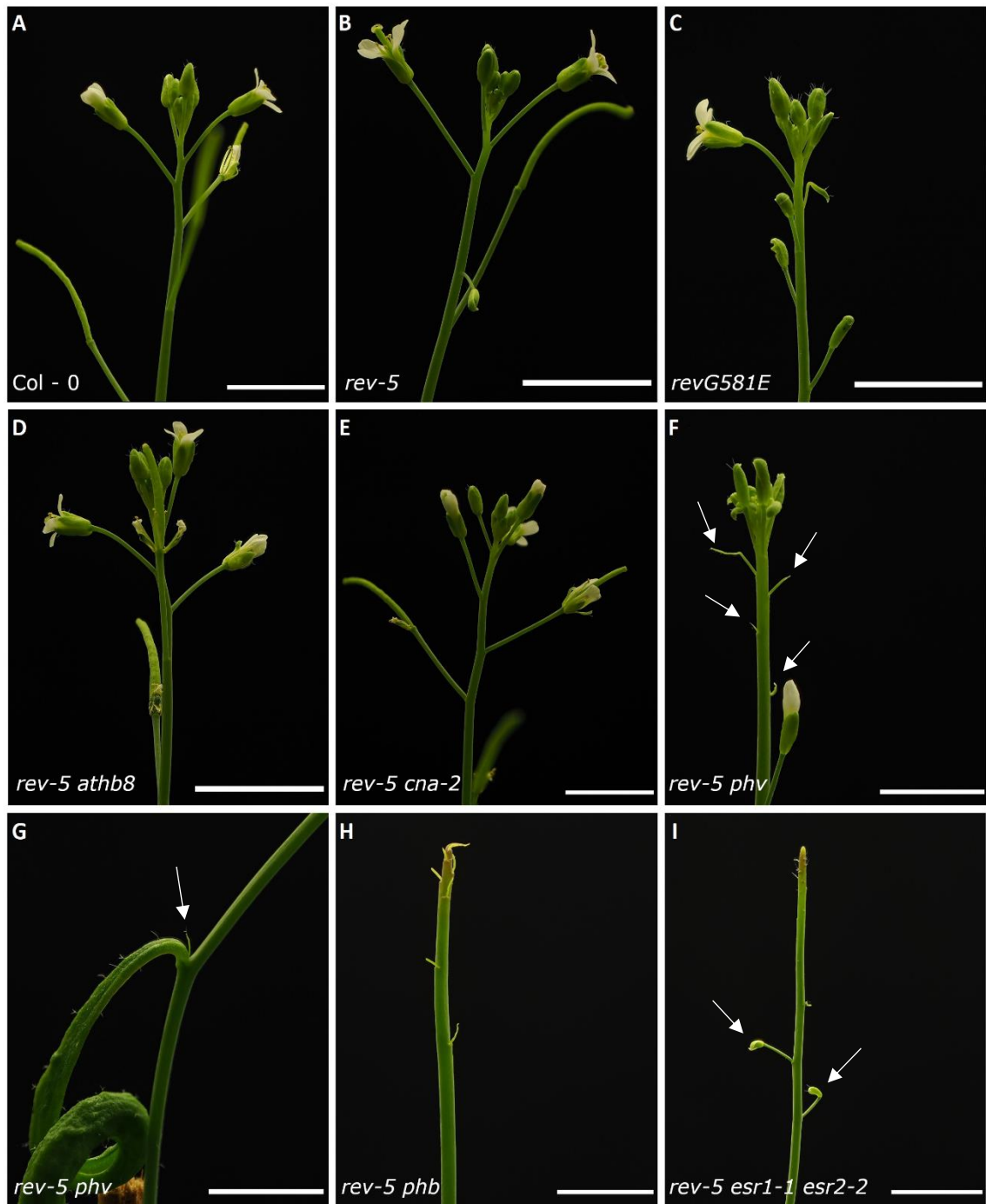


Figure 10 Floral meristems of 30 days old plant. (A) Wild-type, (B) *rev-5*, (C) *revG581E* with small and one arrested floral buds (arrow), (D) *rev-5 athb8* with increased number of flowers, (E) *rev-5 cna-2* also with increased flower count, (F) *rev-5 phv* with filamentous structures in place of inflorescences (arrows), (G) *rev-5 phv* axillary meristem with filament in place of paraclade (arrow), (H) *rev-5 phb* with pin-like apical structure with filaments instead of floral meristems, (I) *rev-5 esr1-1 esr2-2* with apical pin-like structure and two underdeveloped floral buds (arrows). Scale bars = 1cm.

structure was observed in its cauline leaf axils in place of paraclade (Figure 10G). This supports the hypothesis that *PHV* acts in same pathway of AM and FM formation as *REV*.

Both *rev-5 phb* and *rev-5 esr1-1 esr2-2* formed a pin-like structure (62/77 plants and 27/56 plants respectively) (Figure 9) at the top of the stem and produced little to no inflorescences (Figure 10H, I). If flowers were present, they were sterile. The *rev-5 phb* formed filamentous structures instead of inflorescences (Figure 10H) when compared to *rev-5 esr1-1 esr2-2* that produced more floral buds looking structures and only occasionally shorter filaments (Figure 10I). The *rev-5 phv* formed a pin-like structure in 1 of 51 plants (Figure 9).

5 Discussion

The *wus-101 rev-6* pin-like structure phenotype has been previously observed (Otsuga et al., 2001), here we observed same phenotype in *wus-101 rev-5* and also in *wus-101 rev-5 esr1-1* but not in *wus-101 rev-5 esr2-2*. This suggests that the functional *ESR2* protein must be present in order to form this structure. This is supported by similar phenotype observed in *wus-101 esr1-2* where *ESR2* and *REV* wasn't affected. This points to similar function of *ESR1* and *REV*. However, *wus-101 esr1-1* haven't formed a functional meristem, same as *wus-101 rev-5 esr2-2* and *esr1-1 esr2-2*. This shows the importance of *ESR1* and *ESR2* for SAM development.

The *phb phv cna* triple mutant is characteristic by similar phenotype as *clv3* mutant: enlarged SAM, fasciated stem and flowers and multiple cotyledons formation (Prigge et al., 2005). The *wus-101 phb phv cna-2* have been shown to form true leaves from the SAM before its termination and also inflorescences from adventitious meristems through *WUS/CLV3* parallel pathway (Lee and Clark, 2015). The *wus-101 esr1-1 phb phv cna-2* often formed radialized true leaves. They were thicker when compared to radialized structures in *wus-101 rev-5*, *wus-101 esr1-1* and *wus-101 esr1-2*, that were tiny. Moreover, the quintuple mutants had severe cotyledonary defects. The defects of cotyledon formation have been previously described in *esr1* and *esr2* single and double mutants, caused by changes auxin transport (Chandler et al., 2007). In the *wus-101 esr1-1 esr2-2 phb phv cna-2* defects of cotyledons were also observed, but more severe abnormalities were present. The abnormalities included leaf malformations, radialized structures, bulging of the presumptive meristem, duplicated inactive meristem and ultimately complete malformation of the seedling without structured organs.

It has been previously shown that *REV*, *PHB* and *PHV* have overlapping functions in the establishment of SAM (Prigge et al., 2005). Also the enhancement of *rev* phenotype by *phb* and *phv* mutations have been described (Otsuga et al., 2001). Here we described the enhancement of *rev-5* phenotype by *esr1-1 esr2-2* mutations. This indicates that *ESR1* and *ESR2* act redundantly in the same pathway as *REV*, although this enhancement was lower than by *phb* or *phv* mutations. The role of *PHV* in lateral organ development was supported by formation of additional paraclade in place of bract in *phv-1d*. This shows that *PHV* might play a key role in paraclade development. Moreover, cup-shaped leaves have been previously observed in *rev-6 phv* double mutants (Prigge et al., 2005).

However, we did not observe such phenotype in *rev-5 phv*, which shows different effects of *rev-6* allele. Nonetheless, we observed the cup-shaped leaves in *phv-1d* gain-of-function mutants. This shows that *PHV* overexpression might be partially responsible for this phenotype, but it's yet to be elucidated.

We observed increase in AMs from cauline leaves and FMs in *rev-5 athb8* and *rev-5 cna-2* as has previously been observed (Prigge et al., 2005). Nonetheless, the *rev-5 cna-2* formed less rosette leaves than *rev-5*. The role of *ATHB8* and *CNA* is then opposite to the function of *PHB*, *PHV* and *REV* in AM and FM development, but *CNA* acts agonistically to *REV* in terms of rosette leaves development. Although in the *CNA* gain-of-function mutant *icu4-1d* we observed increase in axillary meristem from rosette leaves axils this supports the positive effect of *CNA* on AM development. At the same time the number of rosette leaves was decreased and they were curved upward as observed before (Ochando et al., 2006).

The results of *se-2* were inconclusive, however we could speculate that the abnormal lateral meristem phenotypes were caused by overexpression of all *HD-ZIPIII*s where the paraclade only (C) phenotype appeared at same rate as in *phv-1d* and the bract only (A) appeared at similar rate as in *icu4-1d*.

Figure 11 schematically represents the genetic network of experimentally studied genes in relation with auxin and cytokinin signaling and in relation with other genes having role in the development of the SAM based on the research done. The figure demonstrates that *REV* and *ESR1/2* interact together (line) and together activate meristem through *STM* (Shi et al., 2016; Zhang et al., 2018). *ESR2* however activates *CUC1*, which together with *CUC2* are necessary for *STM* expression (Aida et al., 1999; Ikeda et al., 2006). This shows that *ESR2* activates *STM* in two pathways. *PHB/PHV/CNA* then repress *REV* expression (Williams et al., 2005). It was also suggested that *PHB*, *PHV* and *CNA* might repress meristem functions through *WUS/CLV* pathway (Lee and Clark, 2015), but based on different functions of *CNA* and *PHB/PHV* we suppose that they act in two, yet unclear, separate pathways (dashed block arrows). *PHB* activates *ZPR3*, which leads to *REV* suppression. *ZPR3* has also been shown to suppress all *HD-ZIPIII* members, which is not indicated in the scheme (Wenkel et al., 2007). Role of *ATHB8* isn't indicated because it is still unclear how *ATHB8* affects the SAM, even though it seems that it slightly suppresses the flower phenotype of *rev*, which indicates its opposite role.

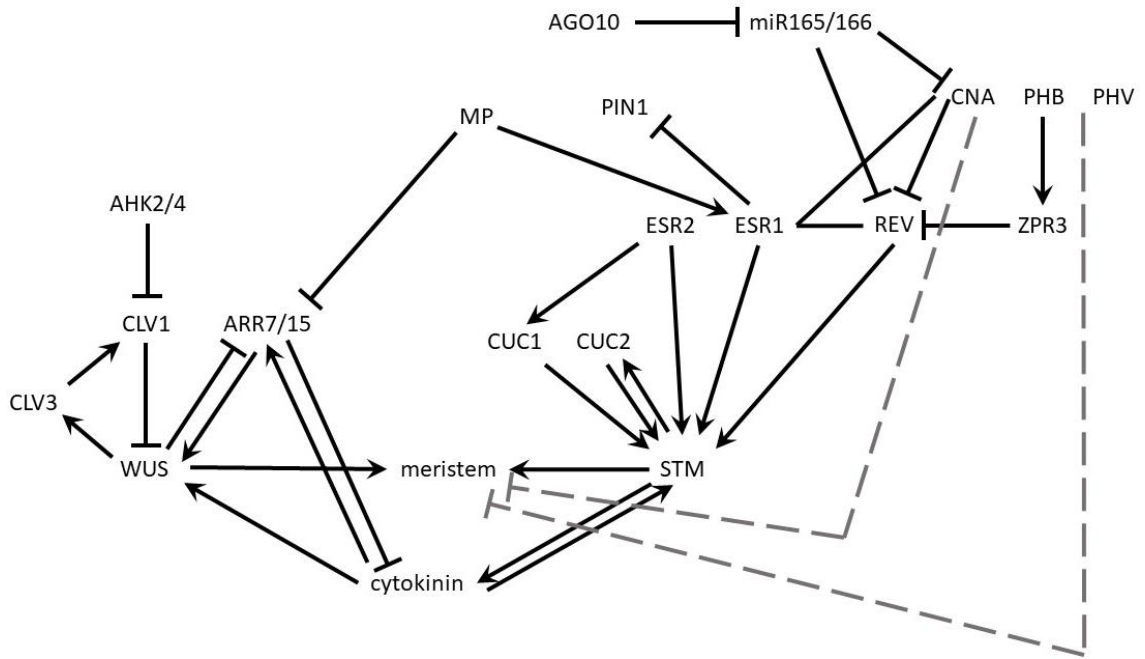


Figure 11 Genetic network of lateral meristem development. Arrows=activation, block arrows=inhibition, dashed grey arrows=two separate pathways of CNA and PHB/PHV mediated inhibition of meristem development. Lines from the sides of ESR1/2 and CNA/PHB/PHV include the whole group.

Cytokinin signaling creates a positive-feedback loop with *STM*, where cytokinin signaling is first activated by *STM* (Yanai et al., 2005). Cytokinin then activates *WUS* transcription directly and also via *AHK2/4* through *CLV1* repression (Gordon et al., 2009). *ARR7/15* activate *WUS* expression, resulting in *ARR7/15* down-regulation by negative-feedback loop which leads to increased cytokinin perception (Argueso et al., 2010; Leibfried et al., 2005). *ARR7/15* are also suppressed by auxin response factor *MP*, causing reduction in *WUS* expression (Zhao et al., 2010). *MP* in turn acts upstream of *ESR1* by positively regulating its expression (Cole et al., 2009) *ESR1* is however responsible for *PIN1* expression patterns (Chandler et al., 2007). This shows the complexity of interactions responsible for proper SAM development.

Based on the similarity between *rev-5 phb*, *rev-5 phv* and *rev-5 esr1-1 esr2-2* we speculate that ESR proteins induce the effects of PHB and PHV, possibly via direct interactions. The *ATHB8* and *CNA* effects should be also induced according to this hypothesis. Then based on our results we propose that *REV*, *PHB* and *PHV* are epistatic to *CNA* and *ATHB8*.

6 Conclusion

In this work we studied the genetic interactions in lateral meristems. We studied the role of *WUS*, *HD-ZIP III* genes and *ESR1/ESR2* in lateral organ development of *A. thaliana* seedlings. We then observed the effect of *HD-ZIP III* and *ESR* genes in *rev* mutant background on lateral organ formation.

We conclude that *ESR* play role as activators of meristem development through *STM* pathway but there might be another, yet unknown pathway for *ESR1/2* actions. The *PHB*, *PHV* and *REV* proteins are responsible for inhibition of meristem growth via *REV* suppression. The *REV* protein binds with *ESR1/2* and together activate *STM*. Up-regulated *REV* with functional *ESR* proteins is then required for the activation of the *WUS*-independent pathway. We confirmed that *PHB*, *PHV* and *REV* have overlapping functions in lateral organ development, although the exact interactions are yet unknown. Additionally, we propose the role of *PHV* in formation of the paraclade structure. This might be caused by *STM* up-regulation, but this yet has to be confirmed. We also showed the opposite roles of *PHB/PHV/REV* and *ATHB/CNA*. Our results however show distinct effects between *ATHB8* and *CNA*. While *CNA* most likely acts as lateral meristem repressor, the role of *ATHB8* and effects of *ESR1/2* binding with *ATHB8* are still unclear.

In the future the auxin signaling could be analyzed in the high order *esr* mutants generated throughout this work and compared with auxin signaling in *HD-ZIP III* gain-of-function mutants. In order to study the *WUS*-independent pathway higher order *hd-zip III* and *esr* mutants with *stm* mutations could be created to elucidate the role of *STM* in this process.

7 References

- Abel, S., Theologis, A., 1996. Early genes and auxin action. *Plant Physiol.* **111**, 9–17.
- Aichinger, E., Kornet, N., Friedrich, T., Laux, T., 2012. Plant stem cell niches. *Annu. Rev. Plant Biol.* **63**, 615–636. <https://doi.org/10.1146/annurev-arplant-042811-105555>
- Aida, M., Ishida, T., Fukaki, H., Fujisawa, H., Tasaka, M., 1997. Genes involved in organ separation in *Arabidopsis*: an analysis of the cup-shaped cotyledon mutant. *Plant Cell* **9**, 841–857. <https://doi.org/10.1105/tpc.9.6.841>
- Aida, M., Ishida, T., Tasaka, M., 1999. Shoot apical meristem and cotyledon formation during *Arabidopsis* embryogenesis: interaction among the CUP-SHAPED COTYLEDON and SHOOT MERISTEMLESS genes. *Dev. Camb. Engl.* **126**, 1563–1570.
- Alonso, J.M., Stepanova, A.N., Leisse, T.J., Kim, C.J., Chen, H., Shinn, P., Stevenson, D.K., Zimmerman, J., Barajas, P., Cheuk, R., Gadriab, C., Heller, C., Jeske, A., Koesema, E., Meyers, C.C., Parker, H., Prednis, L., Ansari, Y., Choy, N., Deen, H., Geralt, M., Hazari, N., Hom, E., Karnes, M., Mulholland, C., Ndubaku, R., Schmidt, I., Guzman, P., Aguilar-Henonin, L., Schmid, M., Weigel, D., Carter, D.E., Marchand, T., Risseuw, E., Brogden, D., Zeko, A., Crosby, W.L., Berry, C.C., Ecker, J.R., 2003. Genome-wide insertional mutagenesis of *Arabidopsis thaliana*. *Science* **301**, 653–657. <https://doi.org/10.1126/science.1086391>
- Anantharaman, V., Aravind, L., 2001. The CHASE domain: a predicted ligand-binding module in plant cytokinin receptors and other eukaryotic and bacterial receptors. *Trends Biochem. Sci.* **26**, 579–582. [https://doi.org/10.1016/S0968-0004\(01\)01968-5](https://doi.org/10.1016/S0968-0004(01)01968-5)
- Argueso, C.T., Raines, T., Kieber, J.J., 2010. Cytokinin signaling and transcriptional networks. *Curr. Opin. Plant Biol.* **13**, 533–539. <https://doi.org/10.1016/j.pbi.2010.08.006>
- Ariel, F.D., Manavella, P.A., Dezar, C.A., Chan, R.L., 2007. The true story of the HD-Zip family. *Trends Plant Sci.* **12**, 419–426. <https://doi.org/10.1016/j.tplants.2007.08.003>
- Banno, H., Ikeda, Y., Niu, Q.W., Chua, N.H., 2001. Overexpression of *Arabidopsis* ESR1 induces initiation of shoot regeneration. *Plant Cell* **13**, 2609–2618. <https://doi.org/10.1105/tpc.010234>
- Bao, N., Lye, K.-W., Barton, M.K., 2004. MicroRNA binding sites in *Arabidopsis* class III HD-ZIP mRNAs are required for methylation of the template chromosome. *Dev. Cell* **7**, 653–662. <https://doi.org/10.1016/j.devcel.2004.10.003>
- Bartel, D.P., 2004. MicroRNAs: Genomics, Biogenesis, Mechanism, and Function. *Cell* **116**, 281–297. [https://doi.org/10.1016/S0092-8674\(04\)00045-5](https://doi.org/10.1016/S0092-8674(04)00045-5)
- Barton, M.K., Poethig, R.S., 1993. Formation of the shoot apical meristem in *Arabidopsis thaliana*: an analysis of development in the wild type and in the shoot meristemless mutant. *Development* **119**, 823–831. <https://doi.org/10.1242/dev.119.3.823>
- Bartrina, I., Otto, E., Strnad, M., Werner, T., Schmülling, T., 2011. Cytokinin Regulates the Activity of Reproductive Meristems, Flower Organ Size, Ovule Formation, and Thus Seed Yield in *Arabidopsis thaliana*. *Plant Cell* **23**, 69–80. <https://doi.org/10.1105/tpc.110.079079>
- Bäurle, I., Laux, T., 2005. Regulation of WUSCHEL Transcription in the Stem Cell Niche of the *Arabidopsis* Shoot Meristem. *Plant Cell* **17**, 2271–2280. <https://doi.org/10.1105/tpc.105.032623>
- Benjamins, R., Quint, A., Weijers, D., Hooykaas, P., Offringa, R., 2001. The PINOID protein kinase regulates organ development in *Arabidopsis* by enhancing polar auxin transport. *Dev. Camb. Engl.* **128**, 4057–4067.
- Bennett, S.R.M., Alvarez, J., Bossinger, G., Smyth, D.R., 1995. Morphogenesis in pinoid mutants of *Arabidopsis thaliana*. *Plant J.* **8**, 505–520. <https://doi.org/10.1046/j.1365-313X.1995.8040505.x>
- Bennett, T., Leyser, O., 2014. The Auxin Question: A Philosophical Overview, in: Zažímalová, E., Petrášek, J., Benková, E. (Eds.), *Auxin and Its Role in Plant Development*. Springer, Vienna, pp. 3–19. https://doi.org/10.1007/978-3-7091-1526-8_1
- Bhatia, N., Bozorg, B., Larsson, A., Ohno, C., Jönsson, H., Heisler, M.G., 2016. Auxin Acts through MONOPTEROS to Regulate Plant Cell Polarity and Pattern Phyllotaxis. *Curr. Biol.* **26**, 3202–3208. <https://doi.org/10.1016/j.cub.2016.09.044>
- Boer, D.R., Freire-Rios, A., van den Berg, W.A.M., Saaki, T., Manfield, I.W., Kepinski, S., López-Vidrieo, I., Franco-Zorrilla, J.M., de Vries, S.C., Solano, R., Weijers, D., Coll, M., 2014.

- Structural Basis for DNA Binding Specificity by the Auxin-Dependent ARF Transcription Factors. *Cell* **156**, 577–589. <https://doi.org/10.1016/j.cell.2013.12.027>
- Bowman, J.L., Eshed, Y., 2000. Formation and maintenance of the shoot apical meristem. *Trends Plant Sci.* **5**, 110–115. [https://doi.org/10.1016/S1360-1385\(00\)01569-7](https://doi.org/10.1016/S1360-1385(00)01569-7)
- Bowman, J.L., Smyth, D.R., Meyerowitz, E.M., 1989. Genes directing flower development in Arabidopsis. *Plant Cell* **1**, 37–52. <https://doi.org/10.1105/tpc.1.1.37>
- Brand, U., Fletcher, J.C., Hobe, M., Meyerowitz, E.M., Simon, R., 2000. Dependence of Stem Cell Fate in Arabidopsis on a Feedback Loop Regulated by CLV3 Activity. *Science* **289**, 617–619. <https://doi.org/10.1126/science.289.5479.617>
- Brand, U., Grünewald, M., Hobe, M., Simon, R., 2002. Regulation of CLV3 Expression by Two Homeobox Genes in Arabidopsis. *Plant Physiol.* **129**, 565–575. <https://doi.org/10.1104/pp.001867>
- Bridge, L.J., Mirams, G.R., Kieffer, M.L., King, J.R., Kepinski, S., 2012. Distinguishing possible mechanisms for auxin-mediated developmental control in Arabidopsis: Models with two Aux/IAA and ARF proteins, and two target gene-sets. *Math. Biosci.* **235**, 32–44. <https://doi.org/10.1016/j.mbs.2011.10.005>
- Busch, W., Miotk, A., Ariel, F.D., Zhao, Z., Forner, J., Daum, G., Suzaki, T., Schuster, C., Schultheiss, S.J., Leibfried, A., Haubeiss, S., Ha, N., Chan, R.L., Lohmann, J.U., 2010. Transcriptional control of a plant stem cell niche. *Dev. Cell* **18**, 849–861. <https://doi.org/10.1016/j.devcel.2010.03.012>
- Carraro, N., Peaucelle, A., Laufs, P., Traas, J., 2006. Cell Differentiation and Organ Initiation at the Shoot Apical Meristem. *Plant Mol. Biol.* **60**, 811–826. <https://doi.org/10.1007/s11103-005-2761-6>
- Chandler, J.W., Cole, M., Flier, A., Grewe, B., Werr, W., 2007. The AP2 transcription factors DORNROSCHEN and DORNROSCHEN-LIKE redundantly control Arabidopsis embryo patterning via interaction with PHAVOLUTA. *Dev. Camb. Engl.* **134**, 1653–1662. <https://doi.org/10.1242/dev.001016>
- Chen, Y., Yordanov, Y.S., Ma, C., Strauss, S., Busov, V.B., 2013. DR5 as a reporter system to study auxin response in Populus. *Plant Cell Rep.* **32**, 453–463. <https://doi.org/10.1007/s00299-012-1378-x>
- Clark, S.E., 1997. Organ Formation at the Vegetative Shoot Meristem. *Plant Cell* **9**, 1067–1076. <https://doi.org/10.1105/tpc.9.7.1067>
- Clark, S.E., Jacobsen, S.E., Levin, J.Z., Meyerowitz, E.M., 1996. The CLAVATA and SHOOT MERISTEMLESS loci competitively regulate meristem activity in Arabidopsis. *Dev. Camb. Engl.* **122**, 1567–1575.
- Clark, S.E., Running, M.P., Meyerowitz, E.M., 1995. CLAVATA3 is a specific regulator of shoot and floral meristem development affecting the same processes as CLAVATA1. *Development* **121**, 2057–2067.
- Clark, S.E., Running, M.P., Meyerowitz, E.M., 1993. CLAVATA1, a regulator of meristem and flower development in Arabidopsis. *Dev. Camb. Engl.* **119**, 397–418.
- Cole, M., Chandler, J., Weijers, D., Jacobs, B., Comelli, P., Werr, W., 2009. DORNROSCHEN is a direct target of the auxin response factor MONOPTEROS in the Arabidopsis embryo. *Development* **136**, 1643–1651. <https://doi.org/10.1242/dev.032177>
- Daum, G., Medzihradsky, A., Suzaki, T., Lohmann, J.U., 2014. A mechanistic framework for noncell autonomous stem cell induction in Arabidopsis. *Proc. Natl. Acad. Sci.* **111**, 14619–14624. <https://doi.org/10.1073/pnas.1406446111>
- Emery, J.F., Floyd, S.K., Alvarez, J., Eshed, Y., Hawker, N.P., Izhaki, A., Baum, S.F., Bowman, J.L., 2003. Radial Patterning of Arabidopsis Shoots by Class III HD-ZIP and KANADI Genes. *Curr. Biol.* **13**, 1768–1774. <https://doi.org/10.1016/j.cub.2003.09.035>
- Endrizzi, K., Moussian, B., Haecker, A., Levin, J.Z., Laux, T., 1996. The SHOOT MERISTEMLESS gene is required for maintenance of undifferentiated cells in Arabidopsis shoot and floral meristems and acts at a different regulatory level than the meristem genes WUSCHEL and ZWILLE. *Plant J. Cell Mol. Biol.* **10**, 967–979. <https://doi.org/10.1046/j.1365-313x.1996.10060967.x>

- Eshed, Y., Izhaki, A., Baum, S.F., Floyd, S.K., Bowman, J.L., 2004. Asymmetric leaf development and blade expansion in Arabidopsis are mediated by KANADI and YABBY activities. *Development* **131**, 2997–3006. <https://doi.org/10.1242/dev.01186>
- Fletcher, J.C., Brand, U., Running, M.P., Simon, R., Meyerowitz, E.M., 1999. Signaling of cell fate decisions by CLAVATA3 in Arabidopsis shoot meristems. *Science* **283**, 1911–1914. <https://doi.org/10.1126/science.283.5409.1911>
- Friml, J., Vieten, A., Sauer, M., Weijers, D., Schwarz, H., Hamann, T., Offringa, R., Jürgens, G., 2003. Efflux-dependent auxin gradients establish the apical-basal axis of Arabidopsis. *Nature* **426**, 147–153. <https://doi.org/10.1038/nature02085>
- Fuchs, M., Lohmann, J., 2020. Aiming for the top: non-cell autonomous control of shoot stem cells in Arabidopsis. *J. Plant Res.* **133**. <https://doi.org/10.1007/s10265-020-01174-3>
- Furutani, M., Vernoux, T., Traas, J., Kato, T., Tasaka, M., Aida, M., 2004. PIN-FORMED1 and PINOID regulate boundary formation and cotyledon development in Arabidopsis embryogenesis. *Dev. Camb. Engl.* **131**, 5021–5030. <https://doi.org/10.1242/dev.01388>
- Gallois, J.-L., Woodward, C., Reddy, G.V., Sablowski, R., 2002. Combined SHOOT MERISTEMLESS and WUSCHEL trigger ectopic organogenesis in Arabidopsis. *Dev. Camb. Engl.* **129**, 3207–3217.
- Giulini, A., Wang, J., Jackson, D., 2004. Control of phyllotaxy by the cytokinin-inducible response regulator homologue ABPHYL1. *Nature* **430**, 1031–1034. <https://doi.org/10.1038/nature02778>
- Gordon, S.P., Chickarmane, V.S., Ohno, C., Meyerowitz, E.M., 2009. Multiple feedback loops through cytokinin signaling control stem cell number within the Arabidopsis shoot meristem. *Proc. Natl. Acad. Sci. U. S. A.* **106**, 16529–16534. <https://doi.org/10.1073/pnas.0908122106>
- Grbić, B., Bleecker, A.B., 1996. An altered body plan is conferred on Arabidopsis plants carrying dominant alleles of two genes. *Dev. Camb. Engl.* **122**, 2395–2403.
- Green, K.A., Prigge, M.J., Katzman, R.B., Clark, S.E., 2005. CORONA, a Member of the Class III Homeodomain Leucine Zipper Gene Family in Arabidopsis, Regulates Stem Cell Specification and Organogenesis. *Plant Cell* **17**, 691–704. <https://doi.org/10.1105/tpc.104.026179>
- Grigg, S.P., Canales, C., Hay, A., Tsiantis, M., 2005. SERRATE coordinates shoot meristem function and leaf axial patterning in Arabidopsis. *Nature* **437**, 1022–1026. <https://doi.org/10.1038/nature04052>
- Guilfoyle, T.J., 2015. The PB1 domain in auxin response factor and Aux/IAA proteins: a versatile protein interaction module in the auxin response. *Plant Cell* **27**, 33–43. <https://doi.org/10.1105/tpc.114.132753>
- Haecker, A., Groß-Hardt, R., Geiges, B., Sarkar, A., Breuninger, H., Herrmann, M., Laux, T., 2004. Expression dynamics of WOX genes mark cell fate decisions during early embryonic patterning in Arabidopsis thaliana. *Development* **131**, 657–668. <https://doi.org/10.1242/dev.00963>
- Hamann, T., Benkova, E., Bäurle, I., Kientz, M., Jürgens, G., 2002. The Arabidopsis BODENLOS gene encodes an auxin response protein inhibiting MONOPTEROS-mediated embryo patterning. *Genes Dev.* **16**, 1610–1615. <https://doi.org/10.1101/gad.229402>
- Harada, J.J., 1999. Signaling in plant embryogenesis. *Curr. Opin. Plant Biol.* **2**, 23–27. [https://doi.org/10.1016/s1369-5266\(99\)80005-3](https://doi.org/10.1016/s1369-5266(99)80005-3)
- Hardtke, C.S., Berleth, T., 1998. The Arabidopsis gene MONOPTEROS encodes a transcription factor mediating embryo axis formation and vascular development. *EMBO J.* **17**, 1405–1411. <https://doi.org/10.1093/emboj/17.5.1405>
- Hazak, O., Bloch, D., Poraty, L., Sternberg, H., Zhang, J., Friml, J., Yalovsky, S., 2010. A Rho Scaffold Integrates the Secretory System with Feedback Mechanisms in Regulation of Auxin Distribution. *PLOS Biol.* **8**, e1000282. <https://doi.org/10.1371/journal.pbio.1000282>
- Hempel, F.D., Zambryski, P.C., Feldman, L.J., 1998. Photoinduction of Flower Identity in Vegetatively Biased Primordia. *Plant Cell* **10**, 1663–1675. <https://doi.org/10.1105/tpc.10.10.1663>
- Hibara, K., Takada, S., Tasaka, M., 2003. CUC1 gene activates the expression of SAM-related genes to induce adventitious shoot formation. *Plant J.* **36**, 687–696. <https://doi.org/10.1046/j.1365-313X.2003.01911.x>

- Holland, C.K., Jez, J.M., 2018. Arabidopsis: the original plant chassis organism. *Plant Cell Rep.* **37**, 1359–1366. <https://doi.org/10.1007/s00299-018-2286-5>
- Hutchison, C.E., Kieber, J.J., 2002. Cytokinin signaling in Arabidopsis. *Plant Cell* **14** Suppl, S47–59. <https://doi.org/10.1105/tpc.010444>
- Hwang, I., Chen, H.-C., Sheen, J., 2002. Two-component signal transduction pathways in Arabidopsis. *Plant Physiol.* **129**, 500–515. <https://doi.org/10.1104/pp.005504>
- Hwang, I., Sheen, J., 2001. Two-component circuitry in Arabidopsis cytokinin signal transduction. *Nature* **413**, 383–389. <https://doi.org/10.1038/35096500>
- Hwang, I., Sheen, J., Müller, B., 2012. Cytokinin signaling networks. *Annu. Rev. Plant Biol.* **63**, 353–380. <https://doi.org/10.1146/annurev-arplant-042811-105503>
- Ikeda, M., Mitsuda, N., Ohme-Takagi, M., 2009. Arabidopsis WUSCHEL Is a Bifunctional Transcription Factor That Acts as a Repressor in Stem Cell Regulation and as an Activator in Floral Patterning. *Plant Cell* **21**, 3493–3505. <https://doi.org/10.1105/tpc.109.069997>
- Ikeda, Y., Banno, H., Niu, Q.-W., Howell, S.H., Chua, N.-H., 2006. The ENHANCER OF SHOOT REGENERATION 2 gene in Arabidopsis regulates CUP-SHAPED COTYLEDON 1 at the transcriptional level and controls cotyledon development. *Plant Cell Physiol.* **47**, 1443–1456. <https://doi.org/10.1093/pcp/pc1023>
- Inoue, T., Higuchi, M., Hashimoto, Y., Seki, M., Kobayashi, M., Kato, T., Tabata, S., Shinozaki, K., Kakimoto, T., 2001. Identification of CRE1 as a cytokinin receptor from Arabidopsis. *Nature* **409**, 1060–1063. <https://doi.org/10.1038/35059117>
- Irish, V.F., Sussex, I.M., 1992. A fate map of the Arabidopsis embryonic shoot apical meristem. *Development* **115**, 745–753. <https://doi.org/10.1242/dev.115.3.745>
- Jasinski, S., Piazza, P., Craft, J., Hay, A., Woolley, L., Rieu, I., Phillips, A., Hedden, P., Tsiantis, M., 2005. KNOX Action in Arabidopsis Is Mediated by Coordinate Regulation of Cytokinin and Gibberellin Activities. *Curr. Biol.* **15**, 1560–1565. <https://doi.org/10.1016/j.cub.2005.07.023>
- Ji, L., Liu, X., Yan, J., Wang, W., Yumul, R.E., Kim, Y.J., Dinh, T.T., Liu, J., Cui, X., Zheng, B., Agarwal, M., Liu, C., Cao, X., Tang, G., Chen, X., 2011. ARGONAUTE10 and ARGONAUTE1 regulate the termination of floral stem cells through two microRNAs in Arabidopsis. *PLoS Genet.* **7**, e1001358. <https://doi.org/10.1371/journal.pgen.1001358>
- Kakimoto, T., 1996. CKI1, a histidine kinase homolog implicated in cytokinin signal transduction. *Science* **274**, 982–985. <https://doi.org/10.1126/science.274.5289.982>
- Kieffer, M., Stern, Y., Cook, H., Clerici, E., Maulbetsch, C., Laux, T., Davies, B., 2006. Analysis of the transcription factor WUSCHEL and its functional homologue in Antirrhinum reveals a potential mechanism for their roles in meristem maintenance. *Plant Cell* **18**, 560–573. <https://doi.org/10.1105/tpc.105.039107>
- Kim, J.-Y., Yuan, Z., Jackson, D., 2003. Developmental regulation and significance of KNOX protein trafficking in Arabidopsis. *Dev. Camb. Engl.* **130**, 4351–4362. <https://doi.org/10.1242/dev.00618>
- Kim, Y.-S., Kim, S.-G., Lee, M., Lee, I., Park, H.-Y., Seo, P.J., Jung, J.-H., Kwon, E.-J., Suh, S.W., Paek, K.-H., Park, C.-M., 2008. HD-ZIP III Activity Is Modulated by Competitive Inhibitors via a Feedback Loop in Arabidopsis Shoot Apical Meristem Development. *Plant Cell* **20**, 920–933. <https://doi.org/10.1105/tpc.107.057448>
- Kirch, T., Simon, R., Grünewald, M., Werr, W., 2003. The DORNROSCHEN/ENHANCER OF SHOOT REGENERATION1 gene of Arabidopsis acts in the control of meristem cell fate and lateral organ development. *Plant Cell* **15**, 694–705. <https://doi.org/10.1105/tpc.009480>
- Laux, T., Mayer, K.F., Berger, J., Jürgens, G., 1996. The WUSCHEL gene is required for shoot and floral meristem integrity in Arabidopsis. *Dev. Camb. Engl.* **122**, 87–96.
- Lee, C., Clark, S.E., 2015. A WUSCHEL-Independent Stem Cell Specification Pathway Is Repressed by PHB, PHV and CNA in Arabidopsis. *PLoS One* **10**, e0126006. <https://doi.org/10.1371/journal.pone.0126006>
- Leibfried, A., To, J.P.C., Busch, W., Stehling, S., Kehle, A., Demar, M., Kieber, J.J., Lohmann, J.U., 2005. WUSCHEL controls meristem function by direct regulation of cytokinin-inducible response regulators. *Nature* **438**, 1172–1175. <https://doi.org/10.1038/nature04270>

- Lenhard, M., Jürgens, G., Laux, T., 2002. The WUSCHEL and SHOOTMERISTEMLESS genes fulfil complementary roles in Arabidopsis shoot meristem regulation. *Development* **129**, 3195–3206. <https://doi.org/10.1242/dev.129.13.3195>
- Leyser, O., 2018. Auxin Signaling. *Plant Physiol.* **176**, 465–479. <https://doi.org/10.1104/pp.17.00765>
- Li, S., Liu, L., Zhuang, X., Yu, Y., Liu, X., Cui, X., Ji, L., Pan, Z., Cao, X., Mo, B., Zhang, F., Raikhel, N., Jiang, L., Chen, X., 2013. MicroRNAs Inhibit the Translation of Target mRNAs on the Endoplasmic Reticulum in Arabidopsis. *Cell* **153**, 562–574. <https://doi.org/10.1016/j.cell.2013.04.005>
- Liu, C., Xu, Z., Chua, N.H., 1993. Auxin Polar Transport Is Essential for the Establishment of Bilateral Symmetry during Early Plant Embryogenesis. *Plant Cell* **5**, 621–630. <https://doi.org/10.1105/tpc.5.6.621>
- Liu, Q., Yao, X., Pi, L., Wang, H., Cui, X., Huang, H., 2009. The ARGONAUTE10 gene modulates shoot apical meristem maintenance and establishment of leaf polarity by repressing miR165/166 in Arabidopsis. *Plant J.* **58**, 27–40. <https://doi.org/10.1111/j.1365-313X.2008.03757.x>
- Lohmann, J.U., Hong, R.L., Hobe, M., Busch, M.A., Parcy, F., Simon, R., Weigel, D., 2001. A Molecular Link between Stem Cell Regulation and Floral Patterning in Arabidopsis. *Cell* **105**, 793–803. [https://doi.org/10.1016/S0092-8674\(01\)00384-1](https://doi.org/10.1016/S0092-8674(01)00384-1)
- Long, J., Barton, M.K., 2000. Initiation of axillary and floral meristems in Arabidopsis. *Dev. Biol.* **218**, 341–353. <https://doi.org/10.1006/dbio.1999.9572>
- Long, J.A., Barton, M.K., 1998. The development of apical embryonic pattern in Arabidopsis. *Dev. Camb. Engl.* **125**, 3027–3035.
- Long, J.A., Moan, E.I., Medford, J.I., Barton, M.K., 1996. A member of the KNOTTED class of homeodomain proteins encoded by the STM gene of Arabidopsis. *Nature* **379**, 66–69. <https://doi.org/10.1038/379066a0>
- Lynn, K., Fernandez, A., Aida, M., Sedbrook, J., Tasaka, M., Masson, P., Barton, M.K., 1999. The PINHEAD/ZWILLE gene acts pleiotropically in Arabidopsis development and has overlapping functions with the ARGONAUTE1 gene. *Dev. Camb. Engl.* **126**, 469–481.
- Maraschin, F. dos S., Memelink, J., Offringa, R., 2009. Auxin-induced, SCF(TIR1)-mediated poly-ubiquitination marks AUX/IAA proteins for degradation. *Plant J. Cell Mol. Biol.* **59**, 100–109. <https://doi.org/10.1111/j.1365-313X.2009.03854.x>
- Mayer, K.F.X., Schoof, H., Haecker, A., Lenhard, M., Jürgens, G., Laux, T., 1998. Role of WUSCHEL in Regulating Stem Cell Fate in the Arabidopsis Shoot Meristem. *Cell* **95**, 805–815. [https://doi.org/10.1016/S0092-8674\(00\)81703-1](https://doi.org/10.1016/S0092-8674(00)81703-1)
- Mayer, U., Ruiz, R.A.T., Berleth, T., Miséra, S., Jürgens, G., 1991. Mutations affecting body organization in the Arabidopsis embryo. *Nature* **353**, 402–407. <https://doi.org/10.1038/353402a0>
- McConnell, J.R., Barton, M.K., 1998. Leaf polarity and meristem formation in Arabidopsis. *Dev. Camb. Engl.* **125**, 2935–2942.
- McConnell, J.R., Barton, M.K., 1995. Effect of mutations in the PINHEAD gene of Arabidopsis on the formation of shoot apical meristems. *Dev. Genet.* **16**, 358–366. <https://doi.org/10.1002/dvg.1020160409>
- Meinke, D.W., Cherry, J.M., Dean, C., Rounsley, S.D., Koornneef, M., 1998. Arabidopsis thaliana: A Model Plant for Genome Analysis. *Science* **282**, 662–682. <https://doi.org/10.1126/science.282.5389.662>
- Meyerowitz, E.M., 1997. Genetic control of cell division patterns in developing plants. *Cell* **88**, 299–308. [https://doi.org/10.1016/s0092-8674\(00\)81868-1](https://doi.org/10.1016/s0092-8674(00)81868-1)
- Mironova, V.V., Omelyanchuk, N.A., Wiebe, D.S., Levitsky, V.G., 2014. Computational analysis of auxin responsive elements in the Arabidopsis thaliana L. genome. *BMC Genomics* **15**, S4. <https://doi.org/10.1186/1471-2164-15-S12-S4>
- Mok, D.W., Mok, M.C., 2001. Cytokinin metabolism and action. *Annu. Rev. Plant Physiol. Plant Mol. Biol.* **52**, 89–118. <https://doi.org/10.1146/annurev.arplant.52.1.89>

- Mougel, C., Zhulin, I.B., 2001. CHASE: an extracellular sensing domain common to transmembrane receptors from prokaryotes, lower eukaryotes and plants. *Trends Biochem. Sci.* **26**, 582–584. [https://doi.org/10.1016/s0968-0004\(01\)01969-7](https://doi.org/10.1016/s0968-0004(01)01969-7)
- Moussian, B., Schoof, H., Haecker, A., Jürgens, G., Laux, T., 1998. Role of the ZWILLE gene in the regulation of central shoot meristem cell fate during Arabidopsis embryogenesis. *EMBO J.* **17**, 1799–1809. <https://doi.org/10.1093/emboj/17.6.1799>
- Mukherjee, K., Bürglin, T.R., 2006. MEKHLA, a Novel Domain with Similarity to PAS Domains, Is Fused to Plant Homeodomain-Leucine Zipper III Proteins. *Plant Physiol.* **140**, 1142–1150. <https://doi.org/10.1104/pp.105.073833>
- Müller, B., Sheen, J., 2008. Cytokinin and auxin interaction in root stem-cell specification during early embryogenesis. *Nature* **453**, 1094–1097. <https://doi.org/10.1038/nature06943>
- Murray, J.A.H., Jones, A., Godin, C., Traas, J., 2012. Systems Analysis of Shoot Apical Meristem Growth and Development: Integrating Hormonal and Mechanical Signaling. *Plant Cell* **24**, 3907–3919. <https://doi.org/10.1105/tpc.112.102194>
- Nishimura, C., Ohashi, Y., Sato, S., Kato, T., Tabata, S., Ueguchi, C., 2004. Histidine Kinase Homologs That Act as Cytokinin Receptors Possess Overlapping Functions in the Regulation of Shoot and Root Growth in Arabidopsis. *Plant Cell* **16**, 1365–1377. <https://doi.org/10.1105/tpc.021477>
- Ochando, I., Jover-Gil, S., Ripoll, J.J., Candela, H., Vera, A., Ponce, M.R., Martínez-Laborda, A., Micol, J.L., 2006. Mutations in the microRNA complementarity site of the INCURVATA4 gene perturb meristem function and adaxialize lateral organs in arabidopsis. *Plant Physiol.* **141**, 607–619. <https://doi.org/10.1104/pp.106.077149>
- Okamoto, J.K., Caster, B., Villarroel, R., Van Montagu, M., Jofuku, K.D., 1997. The AP2 domain of APETALA2 defines a large new family of DNA binding proteins in Arabidopsis. *Proc. Natl. Acad. Sci. U. S. A.* **94**, 7076–7081.
- O'Malley, R.C., Barragan, C.C., Ecker, J.R., 2015. A User's Guide to the Arabidopsis T-DNA Insertion Mutant Collections. *Plant Funct. Genomics* 323–342. https://doi.org/10.1007/978-1-4939-2444-8_16
- Otsuga, D., DeGuzman, B., Prigge, M.J., Drews, G.N., Clark, S.E., 2001. REVOLUTA regulates meristem initiation at lateral positions. *Plant J. Cell Mol. Biol.* **25**, 223–236. <https://doi.org/10.1046/j.1365-313x.2001.00959.x>
- Pouteau, S., Albertini, C., 2011. An assessment of morphogenetic fluctuation during reproductive phase change in Arabidopsis. *Ann. Bot.* **107**, 1017–1027. <https://doi.org/10.1093/aob/mcr039>
- Prigge, M.J., Otsuga, D., Alonso, J.M., Ecker, J.R., Drews, G.N., Clark, S.E., 2005. Class III Homeodomain-Leucine Zipper Gene Family Members Have Overlapping, Antagonistic, and Distinct Roles in Arabidopsis Development. *Plant Cell* **17**, 61–76. <https://doi.org/10.1105/tpc.104.026161>
- Reddy, G.V., Heisler, M.G., Ehrhardt, D.W., Meyerowitz, E.M., 2004. Real-time lineage analysis reveals oriented cell divisions associated with morphogenesis at the shoot apex of *Arabidopsis thaliana*. *Development* **131**, 4225. <https://doi.org/10.1242/dev.01261>
- Reinhardt, D., Pesce, E.-R., Stieger, P., Mandel, T., Baltensperger, K., Bennett, M., Traas, J., Friml, J., Kuhlemeier, C., 2003. Regulation of phyllotaxis by polar auxin transport. *Nature* **426**, 255–260. <https://doi.org/10.1038/nature02081>
- Reinhart, B.J., Weinstein, E.G., Rhoades, M.W., Bartel, B., Bartel, D.P., 2002. MicroRNAs in plants. *Genes Dev.* **16**, 1616–1626. <https://doi.org/10.1101/gad.1004402>
- Rhoades, M.W., Reinhart, B.J., Lim, L.P., Burge, C.B., Bartel, B., Bartel, D.P., 2002. Prediction of Plant MicroRNA Targets. *Cell* **110**, 513–520. [https://doi.org/10.1016/S0092-8674\(02\)00863-2](https://doi.org/10.1016/S0092-8674(02)00863-2)
- Riou-Khamlichi, C., Huntley, R., Jacquard, A., Murray, J.A., 1999. Cytokinin activation of Arabidopsis cell division through a D-type cyclin. *Science* **283**, 1541–1544. <https://doi.org/10.1126/science.283.5407.1541>
- Rodriguez, K., Perales, M., Snipes, S., Yadav, R.K., Diaz-Mendoza, M., Reddy, G.V., 2016. DNA-dependent homodimerization, sub-cellular partitioning, and protein destabilization control WUSCHEL levels and spatial patterning. *Proc. Natl. Acad. Sci. U. S. A.* **113**, E6307–E6315. <https://doi.org/10.1073/pnas.1607673113>

- Rupp, H.M., Frank, M., Werner, T., Strnad, M., Schmülling, T., 1999. Increased steady state mRNA levels of the STM and KNAT1 homeobox genes in cytokinin overproducing *Arabidopsis thaliana* indicate a role for cytokinins in the shoot apical meristem. *Plant J. Cell Mol. Biol.* **18**, 557–563. <https://doi.org/10.1046/j.1365-313x.1999.00472.x>
- Sa, G., Mi, M., He-chun, Y., Ben-ye, L., Guo-feng, L., Kang, C., 2001. Effects of ipt gene expression on the physiological and chemical characteristics of *Artemisia annua* L. *Plant Sci. Int. J. Exp. Plant Biol.* **160**, 691–698. [https://doi.org/10.1016/s0168-9452\(00\)00453-2](https://doi.org/10.1016/s0168-9452(00)00453-2)
- Sakai, H., Honma, T., Aoyama, T., Sato, S., Kato, T., Tabata, S., Oka, A., 2001. ARR1, a transcription factor for genes immediately responsive to cytokinins. *Science* **294**, 1519–1521. <https://doi.org/10.1126/science.1065201>
- Satina, S., Blakeslee, A.F., Avery, A.G., 1940. Demonstration of the Three Germ Layers in the Shoot Apex of *Datura* by Means of Induced Polyploidy in Periclinal Chimeras. *Am. J. Bot.* **27**, 895–905. <https://doi.org/10.2307/2436558>
- Schaller, G.E., 2000. Histidine kinases and the role of two-component systems in plants, in: *Advances in Botanical Research*. Academic Press, pp. 109–148. [https://doi.org/10.1016/S0065-2296\(00\)32023-7](https://doi.org/10.1016/S0065-2296(00)32023-7)
- Schaller, G.E., Kieber, J.J., Shiu, S.-H., 2008. Two-Component Signaling Elements and Histidyl-Aspartyl Phosphorelays†. *Arab. Book Am. Soc. Plant Biol.* **6**. <https://doi.org/10.1199/tab.0112>
- Schauer, S.E., Jacobsen, S.E., Meinke, D.W., Ray, A., 2002. DICER-LIKE1: blind men and elephants in *Arabidopsis* development. *Trends Plant Sci.* **7**, 487–491. [https://doi.org/10.1016/S1360-1385\(02\)02355-5](https://doi.org/10.1016/S1360-1385(02)02355-5)
- Schoof, H., Lenhard, M., Haecker, A., Mayer, K.F., Jürgens, G., Laux, T., 2000. The stem cell population of *Arabidopsis* shoot meristems is maintained by a regulatory loop between the CLAVATA and WUSCHEL genes. *Cell* **100**, 635–644. [https://doi.org/10.1016/s0092-8674\(00\)80700-x](https://doi.org/10.1016/s0092-8674(00)80700-x)
- Sessa, G., Morelli, G., Ruberti, I., 1993. The Athb-1 and -2 HD-Zip domains homodimerize forming complexes of different DNA binding specificities. *EMBO J.* **12**, 3507–3517. <https://doi.org/10.1002/j.1460-2075.1993.tb06025.x>
- Shi, B., Zhang, C., Tian, C., Wang, J., Wang, Q., Xu, T., Xu, Y., Ohno, C., Sablowski, R., Heisler, M.G., Theres, K., Wang, Y., Jiao, Y., 2016. Two-Step Regulation of a Meristematic Cell Population Acting in Shoot Branching in *Arabidopsis*. *PLoS Genet.* **12**. <https://doi.org/10.1371/journal.pgen.1006168>
- Skoog, F., Miller, C.O., 1957. Chemical regulation of growth and organ formation in plant tissues cultured in vitro. *Symp. Soc. Exp. Biol.* **11**, 118–130.
- Smith, R.S., Guyomarc'h, S., Mandel, T., Reinhardt, D., Kuhlemeier, C., Prusinkiewicz, P., 2006. A plausible model of phyllotaxis. *Proc. Natl. Acad. Sci.* **103**, 1301–1306. <https://doi.org/10.1073/pnas.0510457103>
- Smyth, D.R., Bowman, J.L., Meyerowitz, E.M., 1990. Early flower development in *Arabidopsis*. *Plant Cell* **2**, 755–767. <https://doi.org/10.1105/tpc.2.8.755>
- Suzuki, T., Imamura, A., Ueguchi, C., Mizuno, T., 1998. Histidine-containing phosphotransfer (HPt) signal transducers implicated in His-to-Asp phosphorelay in *Arabidopsis*. *Plant Cell Physiol.* **39**, 1258–1268. <https://doi.org/10.1093/oxfordjournals.pcp.a029329>
- Szemenyei, H., Hannon, M., Long, J.A., 2008. TOPLESS Mediates Auxin-Dependent Transcriptional Repression During *Arabidopsis* Embryogenesis. *Science* **319**, 1384–1386. <https://doi.org/10.1126/science.1151461>
- Takei, K., Sakakibara, H., Sugiyama, T., 2001. Identification of genes encoding adenylate isopentenyltransferase, a cytokinin biosynthesis enzyme, in *Arabidopsis thaliana*. *J. Biol. Chem.* **276**, 26405–26410. <https://doi.org/10.1074/jbc.M102130200>
- Talbert, P.B., Adler, H.T., Parks, D.W., Comai, L., 1995. The REVOLUTA gene is necessary for apical meristem development and for limiting cell divisions in the leaves and stems of *Arabidopsis thaliana*. *Dev. Camb. Engl.* **121**, 2723–2735.
- Tan, X., Calderon-Villalobos, L.I.A., Sharon, M., Zheng, C., Robinson, C.V., Estelle, M., Zheng, N., 2007. Mechanism of auxin perception by the TIR1 ubiquitin ligase. *Nature* **446**, 640–645. <https://doi.org/10.1038/nature05731>

- The Arabidopsis Genome Initiative, 2000. Analysis of the genome sequence of the flowering plant *Arabidopsis thaliana*. *Nature* **408**, 796–815. <https://doi.org/10.1038/35048692>
- Tian, C., Zhang, X., He, J., Yu, H., Wang, Y., Shi, B., Han, Y., Wang, G., Feng, X., Zhang, C., Wang, J., Qi, J., Yu, R., Jiao, Y., 2014. An organ boundary-enriched gene regulatory network uncovers regulatory hierarchies underlying axillary meristem initiation. *Mol. Syst. Biol.* **10**, 755. <https://doi.org/10.15252/msb.20145470>
- Ueguchi, C., Koizumi, H., Suzuki, T., Mizuno, T., 2001. Novel family of sensor histidine kinase genes in *Arabidopsis thaliana*. *Plant Cell Physiol.* **42**, 231–235. <https://doi.org/10.1093/pcp/pce015>
- Ulmasov, T., Hagen, G., Guilfoyle, T.J., 1999. Dimerization and DNA binding of auxin response factors. *Plant J. Cell Mol. Biol.* **19**, 309–319. <https://doi.org/10.1046/j.1365-3113x.1999.00538.x>
- Ulmasov, T., Murfett, J., Hagen, G., Guilfoyle, T.J., 1997. Aux/IAA proteins repress expression of reporter genes containing natural and highly active synthetic auxin response elements. *Plant Cell* **9**, 1963–1971. <https://doi.org/10.1105/tpc.9.11.1963>
- Wang, J., Tian, C., Zhang, C., Shi, B., Cao, X., Zhang, T.-Q., Zhao, Z., Wang, J.-W., Jiao, Y., 2017. Cytokinin Signaling Activates WUSCHEL Expression during Axillary Meristem Initiation. *Plant Cell* **29**, 1373–1387. <https://doi.org/10.1105/tpc.16.00579>
- Wang, Q., Kohlen, W., Rossmann, S., Vernoux, T., Theres, K., 2014. Auxin Depletion from the Leaf Axil Conditions Competence for Axillary Meristem Formation in *Arabidopsis* and Tomato. *Plant Cell* **26**, 2068. <https://doi.org/10.1105/tpc.114.123059>
- Wang, Y., Wang, J., Shi, B., Yu, T., Qi, J., Meyerowitz, E.M., Jiao, Y., 2014. The Stem Cell Niche in Leaf Axils Is Established by Auxin and Cytokinin in *Arabidopsis*. *Plant Cell* **26**, 2055–2067. <https://doi.org/10.1105/tpc.114.123083>
- Wenkel, S., Emery, J., Hou, B.-H., Evans, M.M.S., Barton, M.K., 2007. A Feedback Regulatory Module Formed by LITTLE ZIPPER and HD-ZIPIII Genes. *Plant Cell* **19**, 3379–3390. <https://doi.org/10.1105/tpc.107.055772>
- West, A.H., Stock, A.M., 2001. Histidine kinases and response regulator proteins in two-component signaling systems. *Trends Biochem. Sci.* **26**, 369–376. [https://doi.org/10.1016/s0968-0004\(01\)01852-7](https://doi.org/10.1016/s0968-0004(01)01852-7)
- Williams, L., Grigg, S.P., Xie, M., Christensen, S., Fletcher, J.C., 2005. Regulation of *Arabidopsis* shoot apical meristem and lateral organ formation by microRNA miR166g and its AtHD-ZIP target genes. *Development* **132**, 3657–3668. <https://doi.org/10.1242/dev.01942>
- Yadav, R.K., Perales, M., Gruel, J., Girke, T., Jönsson, H., Reddy, G.V., 2011. WUSCHEL protein movement mediates stem cell homeostasis in the *Arabidopsis* shoot apex. *Genes Dev.* **25**, 2025–2030. <https://doi.org/10.1101/gad.17258511>
- Yanai, O., Shani, E., Dolezal, K., Tarkowski, P., Sablowski, R., Sandberg, G., Samach, A., Ori, N., 2005. *Arabidopsis* KNOXI proteins activate cytokinin biosynthesis. *Curr. Biol. CB* **15**, 1566–1571. <https://doi.org/10.1016/j.cub.2005.07.060>
- Zhang, C., Wang, J., Wenkel, S., Chandler, J.W., Werr, W., Jiao, Y., 2018. Spatiotemporal control of axillary meristem formation by interacting transcriptional regulators. *Dev. Camb. Engl.* **145**. <https://doi.org/10.1242/dev.158352>
- Zhao, Z., Andersen, S.U., Ljung, K., Dolezal, K., Miotk, A., Schultheiss, S.J., Lohmann, J.U., 2010. Hormonal control of the shoot stem-cell niche. *Nature* **465**, 1089–1092. <https://doi.org/10.1038/nature09126>

8 List of abbreviations

AGO	ARGONAUTE
AG	AGAMOUS
AHK	<i>Arabidopsis</i> His kinase
AHP	<i>Arabidopsis</i> His phosphotransfer protein
AM	axillary meristem
AP2	APPETALA2
ARE	auxin response element
ARF	AUXIN RESPONSE FACTOR
ARR7/15	ARABIDOPSIS RESPONSE REGULATOR7/15
ATHB8	<i>A. thaliana</i> HOMEODOMAIN8
CLV1/3	CLAVATA1/3
CNA	CORONA
CUC1/2	CUP-SHAPED COTYLEDON1/2
CZ	central zone
EMS	ethyl methanesulfonate
ESR1/2	ENHANCER OF SHOOR REGENERATION1/2
FM	floral meristem
HD-ZIP III	class III homeodomain leucine zipper
HOD1/2	homodimerization domain 1/2
ICU4	INCURVATA4
IPT	ISOPENTENYL TRANSFERASE
MP	MONOPTEROS
OC	organizing center

PHB	PHABULOSA
PHV	PHAVOLUTA
PID	PINOID
PNH	PINHEAD
PZ	peripheral zone
RAM	root apical meristem
REV	REVOLUTA
RISC	RNA-induced silencing complex
RZ	rib zone
SAM	shoot apical meristem
SE	SERRATE
START	steroidogenic acute regulatory protein lipid transfer
STM	SHOOT MERISTEMLESS
T-DNA	transfer-DNA
TPL	TOPLESS
WUS	WUSCHEL
ZPR	LITTLE ZIPPER